

Title: Stimulation-induced changes in diffusion and structure of calmodulin and calmodulin-dependent protein kinase II proteins in neurons

Author: Morteza Heidarinejad, ¹Hideki Nakamura
and Takafumi Inoue

Department of Life Science and Medical Bioscience, School of Advanced Science and Engineering, Waseda University, Tokyo, Japan

¹present address: Department of Cell Biology, School of Medicine, The Johns Hopkins University, Baltimore, MD, USA

E-mail: heidarinejad@gmail.com, hnakamu2@jhmi.edu, and inoue.t@waseda.jp

Correspondence to:

Dr. Takafumi Inoue
Department of Life Science and Medical Bioscience
Waseda University,
2-2 Wakamatsu-cho, Shinjuku,
Tokyo-162-8480, Japan
tel: +81-3-5369-7328
e-mail: inoue.t@waseda.jp

Total number of pages: 57, figures: 12, tables: 2

Abstract

Calcium/calmodulin-dependent protein kinase II (CaMKII) and calmodulin (CaM) play essential roles in synaptic plasticity, which is an elementary process of learning and memory. In this study, fluorescence correlation spectroscopy (FCS) revealed diffusion properties of CaM, CaMKII α and CaMKII β proteins in human embryonic kidney 293 (HEK293) cells and hippocampal neurons. A simultaneous multiple-point FCS recording system was developed on a random-access two-photon microscope, which facilitated efficient analysis of molecular dynamics in neuronal compartments. The diffusion of CaM in neurons was slower than that in HEK293 cells at rest, while the diffusion in stimulated neurons was accelerated and indistinguishable from that in HEK293 cells. This implied that activity-dependent binding partners of CaM exist in neurons, which slow down the diffusion at rest. Diffusion properties of CaMKII α and β proteins implied that major populations of these proteins exist as holoenzymatic forms. Upon stimulation of neurons, the diffusion of CaMKII α and β proteins became faster with reduced particle brightness, indicating drastic structural changes of the proteins such as dismissal from holoenzyme structure and further fragmentation.

Keywords : multi-point fluorescence correlation spectroscopy; molecular diffusion; calmodulin; calmodulin-dependent protein kinase II; neuronal activation

Abbreviations:

AOD: acousto-optic deflector

CaM: calmodulin

CaMKII:	calcium/calmodulin-dependent protein kinase II
FCS:	fluorescence correlation spectroscopy
FRAP:	fluorescence recovery after photobleaching
Glu/Gly:	100 μ M L-glutamate and 10 μ M glycine
HBS:	HEPES-buffered saline
LTP:	long-term potentiation
mCaMKII α :	monomeric CaMKII α
mGFP:	monomeric GFP
NLS:	nuclear localization signal
PBS:	phosphate-buffered saline
RCS:	regulator of calmodulin signaling
TCSPC :	time-correlated single photon counting

Introduction

Calcium/calmodulin-dependent protein kinase II (CaMKII) is one of the most important regulators in synaptic plasticity with its unique functions (Fink and Meyer, 2002; Kerchner and Nicoll, 2008; Lee et al., 2009; Lisman et al., 2002, 2012a). In mammals, four distinct CaMKII proteins, α , β , γ and δ , are encoded by different genes of high homology (Schulman and Hanson, 1993) and more than 30 isoforms are produced by alternative splicing (Brocke et al., 1999; Hudmon and Schulman, 2002a; Lantsman and Tombes, 2005; Rostas and Dunkley, 1992; Takeuchi et al., 2000, 2002). All the four subtypes are expressed in the brain (Hudmon and Schulman, 2002b), whereas the α and β subtypes are the most abundant in the brain, richly found in neurons. CaMKII α transduces Ca²⁺ concentration changes to downstream signals (De Koninck and Schulman, 1998; Hell, 2014; Lisman et al., 2002), while CaMKII β is well known for its ability to bind with F-actin (Sanabria et al., 2009). CaMKII β is also responsible for taking CaMKII α to postsynapse after Ca²⁺ influx (Shen et al., 1998).

The structure of CaMKII proteins consists of three main domains. The N-terminal catalytic domain with kinase activity is followed by the regulatory domain containing an autoinhibitory and a CaM binding sites. A variable linker follows the regulatory domain, in which nuclear localization signal (NLS) is found in some isoforms. By linkage among the C-terminal association domains (Fink and Meyer, 2002), CaMKII proteins form a multimeric structure, holoenzyme, consisting of 6-12 homo- or heteromeric subunits (Hoelz et al., 2003; Kanaseki et al., 1991; Kolodziej et al., 2000; Lantsman and Tombes, 2005). This dodecameric holoenzyme is one of the largest cytosolic proteins of 600 - 660 kDa, approximately 15-35 nm in diameter (Kanaseki et al., 1991; Kolb et al., 1998; Myers et al., 2017). Formation of this

structure induces inter-subunit autophosphorylation at Thr²⁸⁶ of CaMKII α and Thr²⁸⁷ of CaMKII β upon Ca²⁺/CaM binding, which keeps partial CaMKII activity in a Ca²⁺-independent manner long after the initial Ca²⁺ increase event (De Koninck and Schulman, 1998; Hudmon and Schulman, 2002a, 2002b). The holoenzyme formation is thus thought to be essential for proper regulation of CaMKII functions (Shen and Meyer, 1998).

Although CaMKII proteins have been implicated in transmitting signals from plasma membrane, or from postsynapse in the neuron, to nucleus to control gene expression (Coultrap et al., 2011; Ma et al., 2015), the detail is not clear. CaMKII isoforms containing NLS, e.g. α_{β} , γ_A , δ_7 and δ_B , are localized in nucleus (Colbran, 2004; Takeuchi et al., 2002). Phosphorylation of serine residues immediately after the NLS sequence (Heist et al., 1998; Heist and Schulman, 1998) or phosphorylation of Thr²⁸⁶ are implicated in the regulation of nuclear targeting of these CaMKII species (Bayer and Schulman, 2001). Combination of different subunits with or without NLS in a holoenzyme also determines nuclear localization (Srinivasan et al., 1994). Ma et al. proposed that CaMKII γ with an NLS in the variable region serves as a synapse-nuclear messenger by translocating to nucleus upon phosphorylation by CaMKII α and phosphorylates transcription factors and DNA binding proteins, while CaMKII α and β , which lack NLS, play roles in the cytosol (Heist and Schulman, 1998; Ma et al., 2015a).

Calmodulin (CaM) mediates Ca²⁺ signals and modulates activities of numerous signaling proteins. In the neuron, many crucial proteins for synaptic plasticity are targets of CaM (Xia and Storm, 2005). During induction of long-term potentiation (LTP), a conformation change in CaM owing to a relatively large increase in Ca²⁺ allows CaM to activate CaMKII, which

mediates delivery of α -amino-3-hydroxy-5-methyl-4-isoxazolepropionic receptor (AMPA) to the postsynaptic membrane (Hayashi et al., 2000; Lisman et al., 2012b; Lisman and Zhabotinsky, 2001; Merrill et al., 2005). In contrast, induction mechanisms of long-term depression require a small increase in postsynaptic Ca^{2+} , which allows CaM to activate calcineurin (Mulkey et al., 1994; Yasuda et al., 2003). Because the total concentration of CaM-binding proteins is much higher than CaM in the cell, CaM is a limiting factor, whose availability is important in CaM-dependent signaling pathways. It is suggested that the calpacitin protein family sequesters CaM proteins at rest due to its high affinity for CaM at low Ca^{2+} concentrations, in contrast with other CaM targets for which CaM affinities are enhanced by Ca^{2+} binding (Gerendasy, 1999; Xia and Storm, 2005). Thus switching of binding partner of CaM may take place in activity-dependent manners in the neuron.

Altogether, elucidating the dynamics of CaM and CaMKII in both cytosol and nucleus in living neurons is essential in understanding the role of CaM/CaMKII pathway in synaptic plasticity, in relation to short-term and local plasticity within the peri-synaptic region and to the more long-term regulations of transcriptions in the nucleus. In the present study, we focused on diffusion dynamics of CaM and CaMKII in both cytosol and nucleus in HEK293 cells and neurons.

Fluorescence correlation spectroscopy (FCS) has been recruited in the past three decades for analyzing diffusion, binding, concentration, translocation, and conformational changes of bio-molecules due to its suitability for intracellular investigation of bio-molecules (Chen et al., 2008; Haupts et al., 1998; Heikal et al., 2000; Meissner and Häberlein, 2003; Schwille, 2001). In FCS experiments, a finely tuned laser spot within the sample reveals fluorescence intensity

fluctuations via a small number of labeled target molecules passing through the small focal volume, typically less than one femtoliter (Kim et al., 2007; Schwille et al., 1999). Autocorrelation analysis of the fluctuations reveals number, brightness, and the diffusion time of the target molecule species (Müller et al., 2003; Schwille et al., 1999). Compared to similar techniques, such as fluorescence recovery after photobleaching (FRAP) or raster image correlation spectroscopy (RICS), FCS is highly sensitive to lower concentration of the target molecules, with high temporal and spatial resolution (Kim et al., 2010; Meissner and Häberlein, 2003). Therefore, FCS measurement of CaM and CaMKII in living neurons should provide profound insights into their dynamics and physiological roles in synaptic plasticity. However, FCS is basically incompatible with simultaneous recordings from multiple points, for which advanced optical setups are required (Dittrich and Schwille, 2002; Ohsugi and Kinjo, 2009). This drawback can be critical for application in neurons, which are spatially extended with complex morphology and undergo fast biological events such as neuronal activities. To overcome the difficulty, we adopted random-scanning two-photon excitation microscopy (Berland et al., 1995). The random-scanning feature enabled FCS recording from arbitrary multiple points simultaneously, providing an ideal technical platform for FCS measurement in neurons. Multi-point FCS from arbitrary points supersedes line- (Baum et al., 2014; Digman et al., 2005; Ries et al., 2009) and circle- (Petrásek and Schwille, 2008; Ruan et al., 2004) scanning FCS which provide limited flexibility in point selection. The optical plan adopted in this study is much simpler than the multipoint-FCS methods using multiple beams and multiple detectors (Brinkmeier et al., 1999; Dittrich and Schwille, 2002; Ohsugi and

Kinjo, 2009) and spatial light modulators (SLM) (Kloster-Landsberg et al., 2012), in the latter of which cross talk of multiple beams is inherent.

Diffusion is a key element of molecular properties, which determines the activity of cytosolic signaling molecules such as CaM and CaMKII through governing molecular association rate. Diffusion properties of CaM and CaMKII α have been studied using various techniques such as the FRAP (Khan et al., 2012; Lin and Redmond, 2009; Luby-Phelps et al., 1995), FCS (Kim et al., 2004; Sanabria et al., 2008, 2009; Sanabria and Waxham, 2010), image correlation spectroscopy (ICS) (Johnson and Harms, 2016; Sanabria et al., 2008), single molecule tracking (SPT) (Johnson and Harms, 2016), photoactivated localization microscopy (PALM) (Lu et al., 2014), FCS-Förster resonance energy transfer (FCS-FRET) (Lee et al., 2009; Price et al., 2010, 2011) and fluorescence polarization and fluctuation analysis (FPFA) (Nguyen et al., 2015). However, these studies were performed mostly in cell-free media or non-neuronal cells. Although there is a report on a large fraction of mobile CaM in dendritic spines of CA1 hippocampal pyramidal neurons in cultured slices using the FRAP technique (Petersen and Gerges, 2015), quantitative evaluations are still lacking. It is thus largely unknown how the diffusion of these molecules is regulated in neurons, e.g. by neuronal activities. Therefore, we aimed at deciphering diffusion kinetics of CaM and CaMKII in living neurons in conjunction with neuronal activity modulation.

In the present study, we analyzed the diffusion kinetics of CaM and CaMKII proteins in HEK293 cells and in dendrites, cell bodies, and nuclei of neurons. The diffusion of CaM was slower in neurons than in HEK293 cells at rest, while it became similar to that in HEK293 cells upon neuronal activation. This suggests a neuron specific regulation of CaM diffusion

dependent on neuronal activity. CaMKII proteins showed significant increase in diffusion kinetics by neuron stimulation, implying that drastic changes in protein structure took place upon neuronal activation. These results demonstrated feasibility of multipoint FCS in protein dynamics measurement in neurons, as well as complex regulation mechanisms of diffusion properties of CaM and CaMKII during neuronal activities.

Materials and Methods

Cell culture

HEK293 cells. HEK293 cells were grown in Dulbecco's-modified Eagle medium (DMEM) (Nacalai Tesque, Kyoto, Japan) supplemented with 10% fetal bovine serum and 0.05% penicillin/streptomycin (Nacalai Tesque). Cells were plated on coverslips (12 mm in diameter, Matsunami, Tokyo, Japan) coated with Matrigel (BD Bioscience, Tokyo, Japan) 24 hours prior to DNA transfection with Lipofectamine 2000 (Thermo Fisher Scientific, Tokyo, Japan). Cells were subjected to FCS measurement 6–15 hours after transfection in HEPES-buffered saline (HBS, in mM, 20 HEPES, 115 NaCl, 5.4 KCl, 1 MgCl₂, 2 CaCl₂, 10 glucose, pH 7.4).

Dissociated hippocampal neurons and stimulation. Primary cultures from Wistar rat hippocampi were prepared according to a previously described standard method (Bannai et al., 2009). Animal care was in accordance with guidelines outlined by the Institutional Animal Care and Use Committee of Waseda University. All experiments were approved by the Committee on the Ethics of Animal Experiments of Waseda University (2011-A068). All efforts were made to minimize the number of animals used and their suffering during the experiments. Neurons at 7–14 days *in vitro* were transfected with Lipofectamine 2000 and recorded 12–18 hours later. FCS recording was performed in HBS at room temperature. Neurons were stimulated by bath application of 100 μ M L-glutamate (Nacalai Tesque) and 10 μ M glycine (Nacalai Tesque) in HBS (Glu/Gly). In some experiments, Glu/Gly was washed out 20 minutes after stimulation by superfusion of HBS for 5 minutes.

DNA construction

Monomeric GFP (mGFP) (Yang et al., 1996; Zacharias et al., 2002) was fused to target proteins. The CMV promoter of pEGFP-N1 (Takara Bio USA, Mountain View, CA, USA) was internally truncated by about 500 bp to reduce expression (Watanabe and Mitchison, 2002) by digestion of BAL 31 nuclease from the *AatII* site. mGFP vectors, mGFP-N1 and mGFP-C3, were constructed by replacing the enhanced green fluorescence protein (EGFP) sequence of pEGFP-N1 or pEGFP-C3 (Takara Bio USA) with the mGFP sequence of mGFP-CaMKII α (rat CaMKII α , a gift from Dr. Paul De Koninck, Laval University, Quebec, Canada, (Hudmon et al., 2005)) at the *AgeI/BsrGI* sites. mGFP-CaM was constructed by inserting a CaM sequence from pDEST 12.2-CaM (a gift from Dr. Takeo Saneyoshi, Kyoto University, Kyoto, Japan, (Goshima et al., 2008)) into mGFP-C3 at the *BamHI/SacI* sites. CaMKII α -mGFP was constructed by inserting a CaMKII α sequence into mGFP-N1 at the *HindIII/SacII* sites. mGFP-CaMKII β was constructed by replacing the EGFP fragment of gfp-C1-CaMKII β (rat CaMKII β , addgene # 21227, (Shen et al., 1998)) by the mGFP sequence of mGFP-CaMKII α at the *AgeI/HindIII* sites. Monomeric CaMKII α (mCaMKII α) was created by changing a.a. 316 of CaMKII α to a stop codon (Kolb et al., 1998). Other mutants of CaMKII α (I205K, T286A, A302R, T305/306A) were generated by PCR-based point mutagenesis.

FCS

FCS measurements were carried out using a random-scan two-photon microscope equipped with 900 nm Ti:Sapphire laser (Tsunami, Spectra Physics Japan, Tokyo, Japan) as previously described (Shafeghat et al., 2016). All experiments were performed at room

temperature. A 20x water-immersion lens (XLUMPlan FL, N.A. 1.0, Olympus, Tokyo, Japan) was used. Analog output of photon multiplier tubes (PMTs, H7422PA-40, Hamamatsu Photonics, Hamamatsu, Japan) were fed into a time-correlated single photon counting (TCSPC) module (SPC-150, Becker & Hickl, Berlin, Germany) (Becker, 2013). Positions in the X-Y plane were determined by digital commands which were sent from a DAQ interface (NI PCIe-6259, National Instruments, Austin, TX, USA) to the pair of acousto-optic deflector (AOD) devices delivered at 1 MHz maximum. Photon counting through the TCSPC module was synchronized to digital commands to AOD. When FCS was recorded from multiple points, photon counts from each recording point were sorted. Photon counts during the dead time (11.5 μ sec), which were required for the refraction transition of AOD, were discarded.

Before each experiment, optical alignment and calibration were performed using freshly prepared 10 nM Rhodamine 6G (Tokyo Chemical Industry, Tokyo, Japan) in phosphate-buffered saline (PBS). Estimated dimensions of the focal volume of the laser were 0.35 μ m and 3 μ m for radial and axial axes, respectively.

Purified EGFP was used in a cell-free FCS measurement. Histidine-tagged EGFP was expressed in *E. coli*, sonicated, purified with a Ni-NTA resin column in PBS buffer, and eluted with imidazole. Purified EGFP was diluted in PBS at 10 nM and used for FCS.

Laser power was adjusted so as not to saturate absorption (Kim et al., 2007). For intracellular FCS, recording points were chosen after obtaining images by raster scanning. FCS measurements were performed for 15 seconds for 7–15 times from each cellular compartment. Autocorrelation curves were individually calculated from each 15-second record and averaged to produce an autocorrelation result representing the cellular compartment of a

cell. By limiting the fluorescence recording to 15 seconds and averaging the autocorrelation curves obtained from multiple 15-second record chunks, we could eliminate the slow photobleach effect of the total fluorophore population in a cellular compartment. Fluorescence records with no even temporal distribution were omitted. With high expression of fluorescence proteins, excess fluorescence was photobleached by scanning with a high-power laser (5 mW on sample) for 30-60 seconds prior to FCS measurements. The autocorrelation function of each record was calculated after correction of photobleaching decay during the 15-second duration by fitting to a two-component exponential function as follows:

$$G(\tau) = \langle \delta I(t) \cdot \delta I(t + \tau) \rangle / \langle I(t) \rangle^2 \quad (\text{Eq. 1})$$

Autocorrelation functions were obtained from each compartment, i.e., cytosol and nucleus in HEK293 cells; neuronal dendrites, soma, and nucleus of a single neuron, were averaged and fitted to a single- or two-component model of diffusion (Eq. 2) using the Levenberg-Marquardt algorithm (Wohland et al., 2001).

$$G(\tau) = \sum_i C_i \varepsilon_i^2 \cdot G_{Bi} / (V_{eff} (\sum_i C_i \varepsilon_i)^2) \quad (\text{Eq. 2})$$

where $G_{Bi} = (1 + \tau / \tau_{D,i})^{-1} \cdot (1 + \tau / (\gamma^2 \tau_{D,i}))^{-1/2} \cdot G_{(triplet)}(\tau),$

$$\gamma = r_z / r_{xy}, \quad G_{(triplet)}(\tau) = (1 - \theta_T + \theta_T \cdot e^{-\tau/\tau_T}) / (1 - \theta_T)$$

ε_i and C_i represent brightness of each diffusing particle and the concentration of each species, respectively. τ_D represents diffusion time constant, and r_{xy} and r_z represent the radial and axial radii of the laser focal volume. $\Phi_i = \varepsilon_i \times C_i$ serves as the index of total number of chromophores contained in each compartment. Φ_i / Φ_{total} represents the ratio of the number of

labeled molecules in a component against all components; this value differs from C_i / C_{total} when labeled molecules form multimers or become aggregated, thereby indicating the actual molecular distribution among diffusion compartments. We define $\Phi_i / \Phi_{\text{total}}$ as the “molecular distribution ratio” in this paper. The stochastic blinking nature of GFP was incorporated as a triplet term (Haupts et al., 1998). θ_T represents the fraction of particles inside the focal volume, which are in a triplet state with a time constant of τ_T . After fitting the autocorrelation curves of GFP in PBS, τ_T of 0.15 msec was used in recording from all compartments of the cells.

Fitting the results with the two-component model in Eq. 2 resulted in a ratio of ε_1 to ε_2 , not absolute ε_1 and ε_2 . Absolute ε_1 was calculated as follows: average fluorescence intensity of the mixture of the two components is given by $\langle I_t \rangle = \sum_{i=1}^n \langle I_i \rangle$, where $\langle I_i \rangle = \varepsilon_i \cdot N_i$. Applying this definition to the two-component model resulted in the following (Chen et al., 2000):

$$\begin{aligned} \langle I_t \rangle &= \varepsilon_1 \cdot N_1 + \varepsilon_2 \cdot N_2 \\ \langle I_t \rangle &= (\varepsilon_1 \cdot C_1 + \varepsilon_2 \cdot C_2) \cdot V_{\text{eff}} \\ \varepsilon_1 &= \langle I_t \rangle / (V_{\text{eff}}(C_1 + (\varepsilon_2 / \varepsilon_1) \cdot C_2)) \end{aligned} \quad (\text{Eq. 3})$$

C_1 , C_2 , and $\varepsilon_2/\varepsilon_1$ were obtained by fitting to a two-component model of Eq. 2, where $\langle I_i \rangle$ was obtained from the recorded result and ε_1 was calculated by Eq. 3. The ε_i value was inherently affected by the laser power, which changed weekly. When the ε_i values of different molecular species were compared, we conducted a set of experiments in which the laser power was adjusted to a constant value (1.5 mW) at specimens.

In this paper, the diffusion coefficient (D), which was calculated from τ_D and r_{xy} , $D = r_{xy}^2 / (8\tau_D)$ (Kim et al., 2004), is indicated as D_{fast} and D_{slow} for the faster and slower components of a two-component model.

A confocal microscope (FV-300, Olympus) equipped with a 488 nm Argon laser and a water immersion 60x objective (UPlanSApo, N.A. 1.2, Olympus) was used for time-lapse imaging of CaMKII clustering.

Software

All offline analyses were performed using TI Workbench, in-house software written by T.I. running on a Mac computer in combination with Igor Pro (Wave metrics, Lake Oswego, OR, USA) and Microsoft Excel (Microsoft Japan, Tokyo, Japan). All indicated data are given as average \pm SEM. Statistical differences between groups were determined as significant with a confidence level of 95% using the Student's t-tests.

Results

Diffusion of CaM protein in HEK293 cells and neurons

We performed FCS measurements using a custom-built random-scan two-photon laser scan microscope (Shafeghat et al., 2016). The diffusion coefficient (D) of EGFP in cell-free PBS was $77 \mu\text{m}^2/\text{s}$ using our FCS system, which was in accordance with previous reports (78 and $83 \mu\text{m}^2/\text{s}$, respectively) (Chen et al., 2002; Sanabria et al., 2008). We adopted mGFP for a fluorescent tag, because GFP diffuses freely in the cytosol without specific interactions with intracellular milieu (Slade et al., 2009), and mGFP is devoid of dimer assembly known with GFP (Yang et al., 1996; Zacharias et al., 2002). mGFP and mGFP-tagged CaM (mGFP-CaM) were evenly distributed in HEK293 cells, and the fluorescence signal in the nuclei was as high as in the cytosol (Fig. 1A). Autocorrelation functions were calculated from fluorescence fluctuations, which were averaged and then fitted to diffusion models (Fig. 1B–E). Diffusion of proteins generally consists of two distinct populations, fast and slow or immobile components, in intracellular FCS measurements (Merkle et al., 2008). In this study, fitting autocorrelation curves to a one-component diffusion model did not yield acceptable results (Fig. 1D). Therefore, we used a two-component diffusion model. Molecules included in the slower or immobile component diffused ten times slower than in the faster component, probably due to molecular assembly, aggregation, or association with intracellular molecules (Sanabria et al., 2008).

Similar to HEK293 cells, fluorescence intensity of mGFP and mGFP-CaM was similar in the cytosol and nucleus in neurons (Fig. 2A). FCS was conducted in the dendrite, soma, and

nucleus. Autocorrelation functions of mGFP and mGFP-CaM in the cytosol and nucleus of HEK293 cells and in dendrite, soma and nucleus of neurons were calculated (Figs. 1E and 2B) and fitted to the two-component model. Intracellular diffusion of mGFP was 4–5 times slower than diffusion of EGFP in cell-free media. D_{fast} of mGFP-CaM was smaller than that of mGFP in HEK293 cells, which may reflect the difference in molecular mass, as the Stokes-Einstein relation ($D = \frac{kT}{6\pi\eta r}$, where k is Boltzmann's constant, T is absolute temperature, η is viscosity, and r is radius of the spherical particle) suggests that diffusion coefficient of a spherical molecule has inverse relationship to cubic root of molecular mass (Schwille and Haustein, 2006). In neurons, results in the dendrite were similar to the results in soma. D_{fast} of mGFP and mGFP-CaM was similar in the cytosol and nucleus of HEK293 cells, but D_{fast} of mGFP-CaM in neuronal cytosol was smaller than in nucleus and was smaller in neurons than in HEK293 cells (Fig. 2C), which may reflect interactions of CaM molecules with other macromolecules in neurons. These results suggest that binding partners of CaM are abundant in neurons, but not in HEK293 cells. D_{slow} of mGFP-CaM in all neuronal compartments was larger than in HEK293 cells or than D_{slow} of mGFP in neurons, while D_{slow} of mGFP-CaM in HEK293 cells was as small as that of mGFP (Fig. 2D). The molecular distribution ratio of the faster component to all components ($\Phi_{\text{fast}}/\Phi_{\text{total}}$, refer to Materials and Methods) of mGFP and mGFP-CaM was about 90% or more (Fig. 2D and Tables 1 and 2) in all compartments of the both cell types, i.e. about 90% or more molecules were included in the faster component.

Random-scan two-photon microscopy enabled multiple-point FCS

The AOD-driven random scanning mechanism should enable simultaneous multiple-point FCS recording, which has been technically challenging (Brinkmeier et al., 1999; Dittrich and Schwille, 2002; Needleman et al., 2009; Ohsugi and Kinjo, 2009), due to its fast and random scanning feature. In order to demonstrate the multipoint FCS, we compared the multipoint FCS results with those of single-point FCS. There were no significant differences in the shape of autocorrelation curves of mGFP-CaM in the soma of neurons between single-point and two- or three-point FCS (Fig. 3A). Because the fluorescence signal from each recording point was weaker in the multi-point FCS than in the single-point FCS, more records were required to obtain smooth autocorrelation curves (refer to Materials and Methods). In the neuron, two- or three-point FCS in soma and nucleus also resulted in indistinguishable results with one-point FCS records (Fig. 3B and C). Fitting to a two-component diffusion model showed that two- or three-point FCS yielded comparable quantitative diffusion parameters to single-point FCS (Fig. 3D), demonstrating that our multiple-point FCS method can be used to monitor intracellular events from multiple loci in parallel. Therefore, we used multiple- and single-point FCS results intermixed in the following sections.

Diffusion of CaMKII proteins in HEK293 and neurons

We next expressed mGFP-tagged CaMKII α (mGFP-CaMKII α) and CaMKII β (mGFP-CaMKII β) in HEK293 cells and neurons, in which case fluorescence in the nucleus was much dimmer than in the cytosol (Fig. 4A). mGFP-CaMKII α showed diffuse distribution in the cytosol, while mGFP-CaMKII β showed diffuse distribution with a small number of speckles

in the cytosol, as has been reported (Shen and Meyer, 1999). A truncated mutant of CaMKII α (mGFP-mCaMKII α), which lacks the C-terminal association domain thus devoid of forming holoenzyme (Kolb et al., 1998), distributed evenly, and the fluorescence signal in the nuclei was as high as in the cytosol. The difference in the nuclear localization patterns between the truncated mutant of CaMKII α and the full-length versions of CaMKII α and β can be explained by the difference in the molecular mass: the molecular mass of mGFP-mCaMKII α is around 60 kDa, which permits free nuclear pore passage, while the molecular masses of holoenzymes of CaMKII α and β (599 and 633 kDa, respectively (Kanaseki et al., 1991; Kolb et al., 1998)) are too large for passive translocation to nucleus without having an NLS sequence (Ma et al., 2015b; Srinivasan et al., 1994).

Autocorrelation functions were calculated from fluorescence fluctuations (Fig. 4B), which were averaged and fitted to a two-component model. In HEK293 cells, D_{fast} of mGFP-mCaMKII α was significantly smaller than that of mGFP and mGFP-CaM in the cytosol ($p < 0.001$, Table 1). $\Phi_{\text{fast}}/\Phi_{\text{total}}$ of mGFP-mCaMKII α in the cytosol was more than 90% (Fig. 5A and Table 1). Particle brightness of the faster diffusing component (ϵ_{fast}) of mGFP and mGFP-mCaMKII α was similar in both cytosol and nucleus, indicating that the majority of mGFP-mCaMKII α proteins were diffusing without forming multimeric structures, self-aggregation, or association with other molecules (Fig. 5B). CaMKII α and β showed totally different diffusion properties from those of mGFP, CaM and mCaMKII α . The values of D_{fast} of CaMKII α and β in the cytosol were much smaller than those in the nucleus ($p < 0.001$, respectively, Fig. 5A and Table 1) and those of mGFP ($p < 0.001$, respectively), CaM ($p < 0.001$, respectively) and mCaMKII α ($p < 0.001$) in the cytosol. The values of D_{fast} of CaMKII α

and β in the nucleus were within a similar range with that of mCaMKII α . The values of D_{slow} of CaMKII α and CaMKII β in the cytosol were about 10-20 times smaller than D_{fast} (Table 1), which is in accordance with previous reports (Johnson and Harms, 2016). ϵ_{fast} of mCaMKII α in the cytosol was similar to that in the nucleus, while that of CaMKII α was 7.2 ± 0.7 times brighter in the cytosol than in the nucleus (Fig. 5B). The ϵ_{fast} value of CaMKII β was about 7 times brighter in the cytosol than in the nucleus (data not shown), though the laser power was not rigidly adjusted in the case for CaMKII β .

In neurons, the diffusion properties of expressed proteins were similar in the soma and dendrite. mGFP-mCaMKII α diffused faster in the nucleus than in the cytosol (Fig. 4B and 5A and Table 2), suggesting that the mCaMKII α molecules included in the faster diffusing component have more associations with other molecules in the cytosol than in the nucleus, while the difference was not seen in HEK293 cells. $\Phi_{\text{fast}}/\Phi_{\text{total}}$ of mGFP-mCaMKII α in the soma was $90.1 \pm 0.5\%$, indicating that about 90% of these molecules were diffusing as the faster component. ϵ_{fast} of mGFP-mCaMKII α was 1.4 and 1.3 times larger than that of mGFP in the soma and nucleus, respectively, suggesting that the mGFP-mCaMKII α proteins were diffusing in the forms of monomer or dimer (Fig. 5C). D_{fast} of mGFP-CaMKII α and β in the nucleus was larger than that in the soma and dendrite (Fig. 5A and Table 2). While ϵ_{fast} of mGFP-CaMKII α and mGFP-CaMKII β in the nucleus was at similar levels to that of mGFP in the soma and nucleus, ϵ_{fast} of mGFP-CaMKII α and mGFP-CaMKII β in the soma was 6 and 3 times brighter than that in the nucleus, respectively (Fig. 5C and Table 2). When the mGFP tag was fused to the C-terminus of CaMKII α (CaMKII α -mGFP), the features observed with mGFP-CaMKII α , e.g. much smaller D_{fast} and larger ϵ_{fast} in the soma than in the nucleus, were

preserved (Fig. 5A and C). While the ratio of ϵ_{fast} between mGFP-CaMKIIs and mGFP is a good measure of subunit count in single holoenzymes, the value is underestimated due to bleached or unfolded GFP tags of expressed CaMKII subunits and inclusion of endogenous CaMKII subunits. Altogether, in both cell types the faster diffusing components of CaMKII α and β proteins in the cytosol reflect freely diffusing holoenzymes of 6-12 subunits, as is well established, and in the nucleus the faster diffusing component contains totally different molecular forms from holoenzyme.

While ϵ_{slow} of mGFP, CaM and mCaMKII α was twice larger than ϵ_{fast} in the soma ($\epsilon_{\text{slow}}/\epsilon_{\text{fast}} = 1.9 \pm 0.1, 2.3 \pm 0.1$ and 2.1 ± 0.1 , respectively), ϵ_{slow} of CaMKII α and β was more than five times brighter than ϵ_{fast} in the soma (5.4 ± 0.3 and 4.9 ± 0.4 , respectively), which may be interpreted that CaMKII α and β proteins formed aggregated superstructure of holoenzymes in the neuronal cytosol (Fig 5D). About half of CaMKII α and β subunits were included in the slower diffusing component in the cytosol of neurons as $\Phi_{\text{fast}}/\Phi_{\text{total}}$ indicates (Fig. 5A and Table 2), while most of the molecules were included in the faster diffusing component in the nucleus.

Diffusion in stimulated neurons

To investigate how neuronal activity affects the molecular dynamics of mGFP, CaM and CaMKII proteins, neurons were stimulated by bath application of 100 μM L-glutamate and 10 μM glycine (Glu/Gly). mGFP and mGFP-CaM did not show noticeable changes in the diffuse distribution pattern (data not shown). Stimulation accelerated the diffusion of mGFP-CaM in dendrite, soma and nucleus and of mGFP in the soma and nucleus, as autocorrelation curves

apparently shifted to the left (Fig. 6A), and D_{fast} of mGFP and mGFP-CaM increased in all compartments (Fig. 6B) 15 - 25 minutes after the onset of stimulation. The amplitude of increase in D_{fast} of mGFP-CaM was much larger than that of mGFP. The increase of D_{fast} of mGFP may reflect changes in viscosity in the cytosol and nucleus or changes in affinity of mGFP to intracellular macromolecules due to increase in intracellular Ca^{2+} concentration. The larger increase in D_{fast} of mGFP-CaM may be indicating that CaM molecules were liberated from their association partners in addition to the factors that caused the increase in D_{fast} of mGFP. It is unlikely that mGFP-CaM proteins aggregated to form slowly diffusing macromolecular complexes at rest, which dispersed and showed faster mobility upon stimulation, because changes in the particle brightness of the faster diffusing component (ϵ_{fast}) were very small (Fig. 6B). Although the large change in D_{slow} of mGFP-CaM is noticeable, the change in molecular population of the slower diffusion component was minute (5% of the total mGFP-CaM proteins) as $\Phi_{\text{fast}}/\Phi_{\text{total}}$ indicates (Fig. 6B). The changes in diffusion of mGFP and mGFP-CaM peaked at 20 minutes after the start of stimulation. When the stimulant was washed 20 minutes later, the shape of autocorrelation curve and the D_{fast} value returned to the resting levels (Fig. 6C and 7A). This reversible change in the diffusion patterns (Fig. 7) suggest that the diffusion change was not due to protein degradation but rather to re-association with binding partners. Φ_{total} of mGFP-CaM dropped during the stimulation, which contrasts with the flat time course of Φ_{total} of mGFP (Fig. 7C). This could imply that the CaM proteins are degraded during neuronal activation.

CaMKII α and β showed different behaviors from mGFP and mGFP-CaM upon stimulation of neurons. The diffuse distribution pattern of mGFP-CaMKII α was changed to

punctate patterns (Fig. 8A) as has been reported (Dosemeci et al., 2000; Grant et al., 2008; Hudmon et al., 1996, 2005; Shen and Meyer, 1999; Tao-Cheng et al., 2001). The speckles of mGFP-CaMKII α appeared in entire neuronal cytosol but in the nucleus as early as one minute after the stimulation and lasted for one hour until the end of observation without changing the pattern, if the stimulant was not washed, as was reported (Hudmon et al., 2005). The number of CaMKII β speckles was drastically increased by the Glu/Gly stimulation (Fig. 8A) in good accordance to a previous study (Shen and Meyer, 1999). mGFP-mCaMKII α did not show noticeable changes in its diffuse distribution pattern. The stimulation drastically left-shifted autocorrelation functions of mGFP-mCaMKII α , mGFP-CaMKII α , CaMKII α -mGFP and mGFP-CaMKII β in all the three compartments, cell body, dendrite and nucleus, i.e. the diffusion of these proteins was accelerated by the stimulation (Fig. 8B).

To investigate the relationship between the speckle formation and changes in the diffusion properties, mutants of CaMKII α , T286A, I205K, T305/306A and A302R, were expressed in neurons. T286A lacks the kinase activity upon Ca²⁺/CaM binding. A302R lacks affinity to Ca²⁺/CaM and does not form clusters by neuronal stimulation (Barcomb et al., 2015; Nguyen et al., 2015; Shen and Meyer, 1999). The I205K mutation is devoid of any interaction at the T-site of the N-terminal of catalytic domain with the regulatory domain of other CaMKII α subunits or the NR2B subunit of NMDA receptor, thus it lacks aggregation of holoenzyme or association with postsynaptic density proteins (Bayer et al., 2001). The T305/306A mutation prevents the enzyme from secondary phosphorylation at a.a. 305 and 306 and therefore lets the protein bind to Ca²⁺/CaM again after dissociation from CaM (Griffith et al., 2003). All of these mutants showed robust left-shift similarly to that of wild type CaMKII α

by the stimulation, indicating that all of these mutations had no effect on the change in the diffusion property upon stimulation, and thus the speckle formation by stimulation is not directly related to the changes in autocorrelation functions (Fig. 9).

D_{fast} of mCaMKII α , CaMKII α and β was increased in all compartments, and the concentration of proteins was also subjected to change by the stimulation (Fig. 10). The decreases in C_{slow} of CaMKII α and β in the soma and dendrite may reflect the transitions of the slowly diffusing holoenzymes to the faster compartment and to the immobile speckle structures. The overall decrease in total subunit amounts (Φ_{total}) of all the four proteins after the stimulation (Fig. 10B) reflects photobleach, and the relatively large decrease of CaMKII α and β in the soma and dendrite may be attributed to the transition from mobile components to the immobile speckle structure. ϵ_{fast} of CaMKII α and β decreased about 3 and 2 times in the soma, respectively. D_{fast} of CaMKII α and β exceeded $10 \mu\text{m}^2/\text{s}$, which was close to the D_{fast} values of mGFP and mGFP-CaM (Fig. 10A). mCaMKII α showed a slight increase in D_{fast} .

The drastic changes in the shape of autocorrelation function of mGFP-CaMKII α and CaMKII α -mGFP were most prominent at 20 minutes after the start of stimulation (Fig. 11). The change of autocorrelation function of CaMKII α -mGFP was relaxed by the wash of stimulant, but did not return to the initial shape, and that of mGFP-CaMKII α did not recover at all. This not-recovering feature of autocorrelation function made a contrast to the recovery seen in mGFP and mGFP-CaM (Fig. 6C). Diffusion parameters, namely D_{fast} , ϵ_{fast} , ϵ_{slow} and Φ_{total} , showed large changes within 10-20 minutes after stimulation, which did not recover by wash (Fig. 12). The I205K mutant of mGFP-CaMKII α , lacking aggregation of holoenzyme

and association with postsynaptic density proteins (Bayer et al., 2001), showed a similar time course of the diffusion parameters to mGFP-CaMKII α . CaMKII α -mGFP also showed similar time courses of diffusion properties to mGFP-CaMKII α with slower time courses in ϵ_{fast} and ϵ_{slow} : ϵ_{fast} and ϵ_{slow} of it reached the minimum 20 minutes after the stimulation, and those of mGFP-CaMKII α reached the minimum 10 minutes after the stimulation.

Discussion

Molecular dynamics of the mGFP, CaM, CaMKII α and CaMKII β proteins were revealed with the FCS technique in HEK293 cells, which was in accordance with previous studies in non-neuronal cell types (Johnson and Harms, 2016; Khan et al., 2012; Kim et al., 2004; Luby-Phelps et al., 1985; Sanabria et al., 2008). Furthermore, we quantified the dynamics of these proteins in neurons for the first time, which may provide insights into their functions in the neuron. The FCS method clearly showed that CaMKII α and β proteins exist in the cytosol of neurons by forming holoenzyme structures with apparent differences in particle brightness and diffusion constant from monomer forms. Although conventional fluorescence microscopy reports that no, or at most very low, concentration of CaMKII α and CaMKII β proteins in nucleus (Cohen et al., 2015; Ma et al., 2014; Srinivasan et al., 1994) (Fig. 4A), the FCS method reported signals in the nucleus of both HEK293 cells and neurons, the nature of which is discussed below. Stimulation of neurons evoked variety of changes in diffusion properties of the proteins, revealing the effects of neuronal activities on the diffusion properties of these proteins for the first time. While mGFP and CaM showed reversible D_{fast} increase, CaMKII α exhibited irreversible D_{fast} increase. These changes indicate that more or less changes in molecular structure or protein association take place during neuronal activation. We also proved that a time-slicing multiple point FCS measurement is feasible.

Multi-point FCS enabled diffusion measurements in multiple neuronal compartments

In functionally compartmentalized cells such as neurons, it is fundamentally important to read out information in each functional compartment. The conventional FCS method reads

fluorescence fluctuation from a single locus. Dynamic changes in molecular dynamics are expected during neuronal activation, related to various phenomena including synaptic plasticity at postsynapse. In this study, at least three points can be effectively investigated by FCS at the same time. How molecular dynamics are confined or spread in cellular compartments, such as spines, dendritic branches or axon terminals, are important questions in neuroscience, to which 3-point FCS would effectively give answers.

Diffusion of CaM in HEK293 cells and neurons

Through the use of raster image scanning spectroscopy, Sanabria et al. showed that most CaM molecules are involved in molecular complexes in the cytosol and not in the nucleus of HEK293 cells (Sanabria et al., 2008). However, our results showed that most CaM proteins individually diffused in the cytosol and nucleus (Fig. 2D). Sanabria et al. reported that the D -value of EGFP in HEK293 cells was twice as big as CaM in the cytosol and nucleus, while D_{fast} of mGFP was 1.3 and 1.1 times larger than mGFP-CaM, respectively, in this study in HEK293 cells. This discrepancy may be explained by the difference in analysis methods and/or difference in the fluorescent tag: EGFP has a weak dimerization tendency.

CaM exhibited slower diffusion in cytosol of neurons than in HEK293 cells, which may reflect differences in the types and the amount of associating molecules and/or in diffusional obstacles (Sanabria et al., 2007; Zhou et al., 2008). D of CaM has been shown to be reduced from 10 to 7 $\mu\text{m}^2/\text{s}$ in HEK293 cells when CaMKII α was coexpressed, and the slowed CaM diffusion was not affected by a Ca^{2+} increase (Sanabria et al., 2008). In this study, the slow CaM diffusion in the neuronal compartments changed to be as fast as CaM diffusion in

HEK293 cells following the Glu/Gly stimulation. Although CaMKII proteins are abundantly expressed in neurons, CaM may bind to different partners than CaMKII that have higher CaM affinities at rest than in stimulated states. The more than 2-time larger diffusion coefficient of CaM upon stimulation in the neuron than at rest suggested that the CaM binding partners had a several times larger molecular mass than CaM at rest. Although the Ca^{2+} dependency of affinity between calpacitins and CaM, which would be bound at rest and dissociated at high Ca^{2+} (Gerendasy, 1999; Xia and Storm, 2005), is consistent with the observed behavior of CaM diffusion following stimulation, the relatively small molecular sizes of neurogranin (15 kDa) (Watson et al., 1992) and GAP-43 (77 kDa) (Cimler et al., 1985) did not support a simple one-to-one binding of calpacitin proteins to CaM. It is possible that unknown large proteins with a high affinity to Ca^{2+} -free CaM and/or a protein complex containing calpacitins would be present. Our results suggest that a major CaM population was detached from its binding partners upon activation and started to diffuse in cytosol and nucleus, as previously demonstrated (Luby-Phelps et al., 1995). mGFP also showed increase in D_{fast} , which may be ascribed to decrease in viscosity of intracellular milieu or to decrease in nonspecific affinity of intracellular macromolecules to mGFP. The much larger increase in D_{fast} of mGFP-CaM by the stimulation would be explained by changes in affinity of CaM to its binding partners as above in addition to the general mechanisms which increase protein diffusion upon activation seen in the mGFP case. The possibility that degradation of mGFP-CaM during stimulation and alteration of the diffusion coefficient can be rejected by the reversible changes in the D values during stimulation and wash.

A CaM-binding protein, regulator of calmodulin signaling (RCS), is a small 9.6 kDa protein postulated to serve as a CaM inhibitor via sequestration at high Ca^{2+} (Rakhilin et al., 2004). Because the expression level of RCS is low in the hippocampus (Ouimet et al., 1989), small proteins with high affinities to CaM at high Ca^{2+} concentrations could play roles similar to RCS in the hippocampus. Thus, it remains to be elucidated whether CaM proteins diffuse without binding partners or bound by small inhibiting proteins with diffusion constants close to naked forms during neuronal stimulation.

The effects of neuronal activities on the CaMKII diffusion

Upon stimulation with Glu/Gly, CaMKII α and β exhibited drastic changes in their diffusion profiles. mGFP-tagged CaMKII proteins diffused much faster than at rest, which was comparable to the cytosolic diffusion of mGFP, mGFP-CaM and mCaMKII α . The holoenzyme formation of CaMKII α and β was apparently dismissed, as the rapid drop of $\varepsilon_{\text{fast}}$ of CaMKII α proteins indicates (Fig. 12). And each CaMKII subunit seemed to be degraded, because the changes in diffusion properties did not recover after wash (Figs. 11 and 12), which contrasts to the observation that the increase in D_{fast} of mGFP and mGFP-CaM returned to original levels after wash (Figs. 6C and 7A). A possibility that only the mGFP-tag was cleaved and CaMKII α proteins were left intact without fluorescence is unlikely, because both N- and C-terminal tagged CaMKII α proteins showed irreversible increase in D_{fast} by the stimulation.

High intracellular Ca^{2+} levels not only activate CaMKII α but also induce proteolytic activity (Baudry et al., 2015; Goll et al., 2003; Kim et al., 2002; Liu et al., 2006). It has been shown that calpain, a calcium-dependent neutral cysteine protease, cleaves CaMKII α and β

proteins in neurons by NMDA and other stimulants (Hajimohammadreza et al., 1997). Nuclear calpain cleaves CaMKII γ in the nucleus of cerebellar granule cells (Tremper-Wells and Vallano, 2005). The proteolytic activity of calpain is known for LTP formation (Baudry et al., 2013). Digestion of spectrin by calpain facilitates accumulation of glutamate receptors in postsynaptic densities (Baudry et al., 2015). Upon stimulation CaMKII proteins undergo autophosphorylation. It was shown that proteolysis of autophosphorylated CaMKII proteins produces catalytic active fragment of CaMKII of high activity (Kwiatkowski and King, 1989; Yoshimura et al., 1996). The rapid degradation of CaMKII proteins observed in this study could reflect a drastic mobilization of CaMKII upon neuronal stimulation. The loss of CaMKII proteins may be promptly replenished by the well-known rapid RNA synthesis: the CaMKII α gene is classified as an immediate-early gene (Benson et al., 1992; Håvik et al., 2003; Ouyang et al., 1999).

It has been shown that stimulation of neurons with Glu/Gly induces a couple of CaMKII α translocation patterns. CaMKII α is translocated to the postsynaptic region (Otmakhov et al., 2004), where it associates with NMDA-type glutamate receptors and plays important roles in synaptic plasticity (Sanhueza and Lisman, 2013). CaMKII α also forms clusters in the soma and dendrites (Dosemeci et al., 2000; Grant et al., 2008; Hudmon et al., 1996, 2005; Shen and Meyer, 1999; Tao-Cheng et al., 2001) as was seen in this study. A protective role to avoid over-activation of the kinase activity of CaMKII is proposed for this cluster formation (Dosemeci et al., 2000). These translocations may be carried out by CaMKII holoenzymes as a whole. Thus, CaMKII holoenzyme shows different responses to Glu/Gly stimulation,

translocation to postsynapse, cluster formation in the cytosol and degradation, which lead to different consequences.

CaMKII could exist and function in the nucleus

The idea that CaMKII α does not localize in the nucleus has been supported by the nuclear exclusion pattern of CaMKII α in immunohistochemistry and the expression pattern of fluorescent protein-tagged CaMKII α (Cohen et al., 2015; Kutcher et al., 2003; Srinivasan et al., 1994), which was also seen in this study. FCS measurement detected diffusing molecules in the nucleus when mGFP-tagged CaMKII α and β were expressed in both HEK293 cells and primary cultured neurons. Diffusion constant of the molecules in the nucleus was much larger than that in cytosol. There is a possibility that intact monomeric CaMKII α or β exists in the nucleus. Another possibility is that the FCS signal detected in the nucleus derived from degraded mGFP-conjugated CaMKII α or β . Because the resolution of FCS in molecular weight is not high enough to distinguish intact monomeric CaMKII molecules from degraded CaMKII fragments containing a mGFP tag, it is hard to employ either possibilities. However, the intensive degradation of CaMKII upon neuronal stimulation observed in this study implies that fragments of CaMKII proteins resulting from degradation may exist at rest in neurons and HEK293 cells. In either case it is noteworthy that intact monomers or degraded fragments of CaMKII proteins exist in the nucleus, because these forms of CaMKII can retain kinase activity. CaMKII fragments produced from autophosphorylated CaMKII holoenzyme have high kinase activity (Kwiatkowski and King, 1989; Yoshimura et al., 1996). CaMKII γ , which contains NLS, is postulated to transmit postsynaptic information to the nucleus by

translocation (Ma et al., 2014). There is a possibility that CaMKII α and β act as one-time messengers from postsynapse to nucleus by proteolysis.

Conclusion

Since CaM and CaMKII proteins play unique roles in learning and memory, regulation of distribution pattern and molecular structure of these proteins are critically important.

Intriguing properties of CaM and CaMKII proteins in diffusion and assembly were revealed in this study for the first time in living neurons. The apparent changes in CaM protein diffusion by neuronal stimulation implied rapid switching of binding partners of CaM upon neuronal activation. Activity-dependent CaMKII protein degradation was shown to alter the diffusion pattern of the molecule drastically, which raises a possibility of mobilization of CaMKII proteins into active and mobile forms in an irreversible way by neuron stimulation.

Acknowledgement

This work was supported by a Project for Private Universities: matching fund subsidy from MEXT (Ministry of Education, Culture, Sports, Science and Technology) of Japan (T.I.), JSPS KAKENHI Grant Numbers 22650066, 23113515, 23300121, and 26640016 (T.I.). The authors thank Dr. Masataka Kinjo for valuable advice and discussions, Drs. Paul De Koninck and Takeo Saneyoshi for the gift of plasmids, and Mr. Kenta Saito for technical assistance.

Tables

Table 1. D_{fast} , D_{slow} , Φ_{fast}/Φ_{total} and ϵ_{fast} of mGFP, mGFP-CaM, mGFP-mCaMKII α , mGFP-CaMKII α and mGFP-CaMKII β proteins in the cytosol and nucleus of HEK293 cells.

Protein	n (cell)	D_{fast} ($\mu\text{m}^2/\text{s}$)	D_{slow} ($\mu\text{m}^2/\text{s}$)	Φ_{fast}/Φ_{total} (%)	ϵ_{fast} (a.u.)
mGFP					
Cytosol	18	17.0 ± 0.7	0.07 ± 0.01	92.4 ± 1.4	86 ± 13 (n=5)
Nucleus	13	14.4 ± 0.6	0.08 ± 0.01	93.5 ± 1.8	95 ± 14 (n=5)
mGFP-CaM					
Cytosol	5	12.9 ± 0.9	0.10 ± 0.02	93.4 ± 1.0	
Nucleus	9	12.9 ± 0.8	0.12 ± 0.02	95.8 ± 0.6	
mGFP-mCaMKIIα					
Cytosol	12	8.2 ± 0.6	0.11 ± 0.02	89.1 ± 1.4	90 ± 5 (n=7)
Nucleus	15	8.8 ± 0.9	0.13 ± 0.02	89.5 ± 1.5	78 ± 7 (n=7)
mGFP-CaMKIIα					
Cytosol	11	3.9 ± 0.4	0.53 ± 0.06	63.8 ± 5.3	545 ± 108 (n=7)
Nucleus	11	9.0 ± 0.8	0.19 ± 0.02	81.2 ± 1.3	73 ± 8 (n=7)
mGFP-CaMKIIβ					
Cytosol	14	3.0 ± 0.2	0.27 ± 0.04	67.7 ± 4.8	
Nucleus	13	8.9 ± 0.8	0.18 ± 0.03	85.3 ± 1.6	

The values were calculated by fitting the autocorrelation curves to a two-component diffusion model. Laser power was adjusted to the same level in the experiments measuring the ϵ values. Results of single cell were calculated and averaged. Average \pm S.E.M is indicated.

Table 2. D_{fast} , D_{slow} , Φ_{fast}/Φ_{total} and \mathcal{E}_{fast} of mGFP, mGFP-CaM, mGFP-mCaMKII α , mGFP-CaMKII α , CaMKII α -mGFP and mGFP-CaMKII β proteins in the dendrite, soma and nucleus of hippocampal neurons.

Protein	n (cell)	D_{fast} ($\mu\text{m}^2/\text{s}$)	D_{slow} ($\mu\text{m}^2/\text{s}$)	Φ_{fast}/Φ_{total} (%)	\mathcal{E}_{fast} (a.u.)
mGFP					
Dendrite	10	13.8 ± 0.9	0.10 ± 0.02	93.0 ± 1.1	
Soma	25	14.2 ± 0.5	0.12 ± 0.02	92.5 ± 0.7	69 ± 4 (n=7)
Nucleus	22	16.2 ± 0.7	0.14 ± 0.02	93.7 ± 0.7	69 ± 3 (n=7)
mGFP-CaM					
Dendrite	34	7.6 ± 0.5	0.27 ± 0.04	88.9 ± 0.6	
Soma	45	7.8 ± 0.5	0.27 ± 0.02	89.0 ± 0.7	75 ± 4 (n=4)
Nucleus	33	9.2 ± 0.5	0.28 ± 0.04	91.7 ± 0.6	75 ± 3 (n=4)
mGFP-mCaMKIIα					
Dendrite	34	7.5 ± 0.4	0.24 ± 0.04	88.1 ± 0.9	
Soma	38	6.6 ± 0.3	0.25 ± 0.03	90.1 ± 0.5	90 ± 10 (n=11)
Nucleus	37	9.4 ± 0.7	0.25 ± 0.04	90.8 ± 0.5	83 ± 12 (n=11)
mGFP-CaMKIIα					
Dendrite	36	5.9 ± 0.4	0.30 ± 0.03	47.2 ± 2.2	
Soma	41	5.6 ± 0.4	0.27 ± 0.02	52.0 ± 2.0	315 ± 40 (n=19)
Nucleus	19	9.2 ± 1.3	0.16 ± 0.02	80.3 ± 2.1	52 ± 5 (n=19)
CaMKIIα-mGFP					
Soma	6	4.3 ± 0.2	0.28 ± 0.04	62.2 ± 2.7	338 ± 34 (n=6)
Nucleus	6	8.0 ± 0.5	0.22 ± 0.05	85.5 ± 2.9	78 ± 7 (n=6)
mGFP-CaMKIIβ					
Dendrite	24	5.9 ± 0.6	0.26 ± 0.05	47.6 ± 2.7	
Soma	27	5.7 ± 0.5	0.22 ± 0.03	58.7 ± 2.4	136 ± 16 (n=12)
Nucleus	19	10.8 ± 1.1	0.11 ± 0.02	82.0 ± 1.9	48 ± 5 (n=12)

The values were calculated by fitting the autocorrelation curves to a two-component diffusion model. Laser power was adjusted to the same level in the experiments measuring the \mathcal{E} values. Results of single cells were calculated and averaged. Average \pm S.E.M is indicated.

Figure legends

Fig 1. Expression of mGFP and mGFP-CaM in HEK293 cells and FCS measurements.

(A) Fluorescence images of HEK293 cells transfected with mGFP (a) and mGFP-CaM (b). **Scale bar**, 10 μm . (B) Time course of photon counts recorded at 100 kHz from a single point in a HEK293 cell expressing mGFP-CaM. Inset, an expanded view. (C) Overlay of normalized autocorrelation functions of seven traces recorded from the cytosol of an mGFP-CaM expressing HEK293 cell. (D) Fitting results with one- and two-component models of the averaged autocorrelation function shown in C. The residual of fitting (**gray lines**) indicates that the two-component model is better than the one-component model. Bottom boxes show expanded views. **Marks**, autocorrelation function; **red lines**, fitting results. (E) Normalized averaged autocorrelation functions of mGFP and mGFP-CaM in cytosol and nucleus of HEK293 cells. Circles and lines indicate autocorrelation functions and fitted results, respectively. Autocorrelation functions in each single cell were averaged, then the averages of all cells were averaged.

Fig 2. Expression of mGFP and mGFP-CaM in hippocampal neurons and quantitative FCS analysis.

(A) Fluorescence images of neurons transfected with mGFP (a) and mGFP-CaM (b). **Scale bar**, 20 μm . (B) Averaged autocorrelation functions of mGFP and mGFP-CaM taken in soma, dendrite and nucleus of neurons. Autocorrelation functions of records in a single cell were averaged, then averages of all cells were averaged. (C) Averaged autocorrelation functions of mGFP-CaM from HEK293 cells and neurons are compared. Data used in Figs.

1E and 2B are shown. **(D)** D_{fast} , D_{slow} , Φ_{fast}/Φ_{total} and $\epsilon_{slow}/\epsilon_{fast}$ of mGFP and mGFP-CaM proteins in the soma and dendrite (**den**) of neurons, cytosol of HEK293 cells (**cyto**), and nucleus (**nuc**), were calculated by fitting to a two-component diffusion model. Each result of a single cell is indicated by a dot, and averages and SEMs are indicated by bars and error bars, respectively (* $P < 0.05$, ** $P < 0.01$ and *** $P < 0.001$, Student's t-test).

Fig 3. Multiple-point FCS.

(A) Autocorrelation curves constructed by one- (**red**), two- (**green**), and three-point (**blue**) measurements of mGFP-CaM in the soma of a neuron. **(B and C)** Comparison of autocorrelation curves between one- and two- (**B**) or three-point (**C**) simultaneous FCS recordings from the same cells. Autocorrelation curves of mGFP-CaM were taken in dendrite, soma, and nucleus of hippocampal neurons. Autocorrelation functions in each single cell were averaged, then the averages of all cells were averaged. **(D)** Comparison of one- and two-point (**left**) and one- and three-point (**right**) FCS measurement. D_{fast} and D_{slow} of mGFP-CaM proteins in dendrite (**den**), soma, and nucleus (**nuc**) of neurons were calculated by fitting to a two-component diffusion model. Each result of a single cell is indicated by a dot, and averages and SEMs are indicated by bars and error bars, respectively.

Fig 4. Expression of mGFP-mCaMKII α , mGFP-CaMKII α and mGFP-CaMKII β in HEK293 cells and hippocampal neurons and FCS measurements.

(A) Fluorescence images of HEK293 cells and hippocampal neurons transfected with mGFP-mCaMKII α , mGFP-CaMKII α , and mGFP-CaMKII β . **Scale bars**, 10 μm (**a-c**) and 20

μm (**d-f**). **(B)** Normalized averaged autocorrelation functions of mGFP-mCaMKII α , mGFP-CaMKII α , and mGFP-CaMKII β in soma (**red**), dendrite (**blue**), and nucleus (**green**) of neurons, and in cytosol (**red**) and nucleus (**green**) of HEK293 cells, and CaMKII α -mGFP in soma (**red**), and nucleus (**green**) of neurons. Autocorrelation functions in each single cell were averaged, then the averages of all cells were averaged. CaMKII α and β showed apparently faster diffusion in the nucleus than in soma and dendrite.

Fig. 5. Quantitative analysis of FCS measurements on CaMKII proteins.

(A) D_{fast} , D_{slow} , and $\Phi_{\text{fast}}/\Phi_{\text{total}}$ of mGFP-mCaMKII α , mGFP-CaMKII α , mGFP-CaMKII β , and CaMKII α -mGFP proteins in cytosol (**cyto**) and nucleus (**nuc**) of HEK293 cells and in soma, dendrite (**den**), and nucleus (**nuc**) of neurons were calculated by fitting to a two-component diffusion model. **(B and C)** The ϵ_{fast} values of mGFP, mGFP-mCaMKII α , and mGFP-CaMKII α in cytosol (**cyto**) and nucleus (**nuc**) of HEK293 cells (**B**) and of mGFP, mGFP-mCaMKII α , mGFP-CaMKII α , mGFP-CaMKII β and CaMKII α -mGFP in soma and nucleus (**nuc**) of neurons (**C**) are shown. The ϵ_{fast} values of CaMKII α in cytosol (**cyto** and **soma**) were much larger than those in nucleus and those of mGFP and mGFP-mCaMKII α , suggesting that CaMKII α formed multimeric structure of more than five subunits only in cytosol. Laser power was adjusted to the same level in the experiments among which the ϵ value were compared. **(D)** $\epsilon_{\text{slow}}/\epsilon_{\text{fast}}$ of mGFP, mGFP-CaM, mGFP-mCaMKII α , mGFP-CaMKII α , mGFP-CaMKII β , and CaMKII α -mGFP in soma of neurons are shown. Each result of a single cell is indicated by a dot, and averages and SEMs are indicated by bars and error bars, respectively (* $P < 0.05$, ** $P < 0.01$, *** $P < 0.001$, Student's t-test).

Fig 6. Effect of neuronal activation on the dynamics of mGFP and mGFP-CaM in neurons.

(A) Normalized autocorrelation functions of mGFP and mGFP-CaM before (**black**) and after (**red**) stimulation with 100 μ M Glu/10 μ M Gly in dendrite, soma, and nucleus of neurons. In all compartments, autocorrelation functions shifted to the left after the stimulation (15 - 25 minutes after the onset of stimulation). Autocorrelation functions of records in each single cell were averaged first, then averages of all cells were averaged. (B) D_{fast} , D_{slow} , ϵ_{fast} , ratio of changes in ϵ_{fast} , and Φ_{fast}/Φ_{total} before and after the stimulation. Data of after stimulation were taken from 15 to 25 minutes after the stimulation. Results from each single cell are indicated by dots, and averages and SEMs are shown by bars and error bars, respectively (* $P < 0.05$, ** $P < 0.01$, Student's paired t-test). 'b' and 'a' denote before and after, respectively. (C) Time courses of autocorrelation functions of mGFP-CaM and mGFP during stimulation and after wash are shown. The stimulant was washed 20 minutes after the onset of stimulation. The left-shift of the autocorrelation curves peaked at 10 minutes, gradually shifted back to the right, and returned to the resting level after wash. Marks indicate averaged autocorrelation functions from 8 (mGFP) and 7 (mGFP-CaM) cells, and lines show fit results.

Fig. 7. Time course FCS parameters of mGFP and mGFP-CaM before and after stimulation in soma of neurons.

Time courses of D_{fast} and D_{slow} (A), ϵ_{fast} and ϵ_{slow} (B), and Φ_{fast}/Φ_{total} and Φ_{total} (C) of mGFP (n=8) and mGFP-CaM (n=7) before and after stimulation are shown. Stimulant was

washed 20 minutes after the onset of stimulation. D_{fast} was increased during stimulation, and turned back to the original level after wash.

Fig. 8. Effect of neuronal activation on the dynamics of CaMKII in neurons.

(A) Fluorescence images of neurons transfected with mGFP-mCaMKII α , mGFP-CaMKII α , and mGFP-CaMKII β before (0 min) and 2, 15 and 25 minutes after stimulation with 100 μ M Glu/10 μ M Gly. Speckle patterns of mGFP-CaMKII α and mGFP-CaMKII β appeared at 2 minutes, which became more obvious at 15 and 25 minutes. **Scale bar**, 4 μ m. (B) Normalized autocorrelation functions of mGFP-mCaMKII α , mGFP-CaMKII α , CaMKII α -mGFP, and mGFP-CaMKII β before (**black**) and after (**red**) stimulation in soma, dendrite, and nucleus. Autocorrelation functions in each single cell were averaged first, then the averages of all cells were averaged and indicated. All autocorrelation functions shifted to the left by the stimulation.

Fig. 9. Changes in distribution patterns and autocorrelation functions of CaMKII α mutants by Glu/Gly stimulation.

CaMKII α mutants, T286A, T305/306A, I205K, and A302R, tagged with mGFP at N-termini were expressed in hippocampal neurons and stimulated with Glu/Gly (n=3 for T286A, T305/306A, and A302R and n=9 for I205K). Fluorescence images indicate appearance of speckled patterns in neurons expressing the T286A and T305/306A mutants by the stimulation, but not in neurons expressing the I205K and A302R mutants. In contrast, autocorrelation functions of all these mutants in the soma shifted to the left. The

data of after stimulation were taken between 15 to 25 min after the onset of stimulation. Autocorrelation functions of records in each single cell were averaged first, then the averages of all cells were averaged and indicated. **Scale bar**, 10 μm .

Fig. 10. Changes in FCS parameters evoked by Glu/Gly stimulation.

D_{fast} , C_{fast} , and C_{slow} of mGFP-mCaMKII α , mGFP-CaMKII α , mGFP-CaMKII β , and CaMKII α -mGFP proteins (**A**), and ratios of ϵ_{fast} and Φ_{total} of mGFP-mCaMKII α , mGFP-CaMKII α , mGFP-CaMKII β and CaMKII α -mGFP proteins (**B**) before and after stimulation are shown. Data were taken before and between 15 to 25 minutes after the onset of stimulation. ϵ_{fast} of mGFP-CaMKII α and CaMKII α -mGFP in dendrite and soma was decreased by three-fold by the stimulation. In (**A**), 'b' and 'a' denote before and after, respectively. Each result of a single cell is indicated by a dot, and averages and SEMs are indicated by bars and error bars, respectively (* $p < 0.05$, ** $p < 0.01$, *** $p < 0.001$, Student's paired t-test). In **B** statistical tests were performed between the values before and after the simulation, and statistical significance is marked on corresponding bars.

Fig. 11. Time course of autocorrelation functions of mGFP-mCaMKII α , mGFP-CaMKII α , and CaMKII α -mGFP in stimulated neurons.

Time courses of autocorrelation function of mGFP-CaMKII α (**A**, $n=7$), CaMKII α -mGFP (**B**, $n=6$) and mGFP-mCaMKII α (**C**, $n=5$) during stimulation and after wash are shown. The Glu/Gly stimulation solution was washed 20 minutes after the onset of stimulation. The left-shift of the autocorrelation curves peaked at 20 minutes and did not recover after wash. Dots

indicate autocorrelation functions at each τ , and lines show fitting results. Autocorrelation functions of records in each time point were averaged.

Fig. 12. Time course of FCS parameters of mGFP-CaMKII α protein before and after stimulation in soma of neurons.

Time courses of D_{fast} , D_{slow} (**A**), ϵ_{fast} and ϵ_{slow} (**B**), C_{fast} and C_{slow} (**C**) and Φ_{total} (**D**) of mGFP-CaMKII α (n=7), mGFP-CaMKII α (I205K) (n=6) and CaMKII α -mGFP (n=6) proteins before and after stimulations are shown. Stimulant was washed 20 min after stimulation. The increases of D_{fast} and decreases of ϵ_{fast} of the proteins imply break-down of the holoenzyme structure of CaMKII α during stimulation. There were no apparent differences in these FCS parameters among mGFP-CaMKII α , mGFP-CaMKII α (I205K) and CaMKII α -mGFP proteins.

References

- Bannai, H., Lévi, S., Schweizer, C., Inoue, T., Launey, T., Racine, V., Sibarita, J.-B., Mikoshiba, K., Triller, A., 2009. Activity-dependent tuning of inhibitory neurotransmission based on GABAAR diffusion dynamics. *Neuron* 62, 670–682.
<https://doi.org/10.1016/j.neuron.2009.04.023>
- Barcomb, K., Goodell, D.J., Arnold, D.B., Bayer, K.U., 2015. Live imaging of endogenous Ca²⁺/calmodulin-dependent protein kinase II in neurons reveals that ischemia-related aggregation does not require kinase activity. *J. Neurochem.* 135, 666–673.
<https://doi.org/10.1111/jnc.13263>
- Baudry, M., Chou, M.M., Bi, X., 2013. Targeting calpain in synaptic plasticity. *Expert Opin. Ther. Targets* 17, 579–592. <https://doi.org/10.1517/14728222.2013.766169>
- Baudry, M., Zhu, G., Liu, Y., Wang, Y., Briz, V., Bi, X., 2015. Multiple cellular cascades participate in long-term potentiation and in hippocampus-dependent learning. *Brain Res.* 1621, 73–81. <https://doi.org/10.1016/j.brainres.2014.11.033>
- Baum, M., Erdel, F., Wachsmuth, M., Rippe, K., 2014. Retrieving the intracellular topology from multi-scale protein mobility mapping in living cells. *Nat. Commun.* 5, 4494.
<https://doi.org/10.1038/ncomms5494>
- Bayer, K.U., De Koninck, P., Leonard, A.S., Hell, J.W., Schulman, H., 2001. Interaction with the NMDA receptor locks CaMKII in an active conformation. *Nature* 411, 801–805.
<https://doi.org/10.1038/35081080>
- Becker, 2013. *TCSPC Handbook*. 5th ed. Berlin. Becker and Hickl GmbH.
- Benson, D.L., Gall, C.M., Isackson, P.J., 1992. Dendritic localization of type II calcium calmodulin-dependent protein kinase mRNA in normal and reinnervated rat hippocampus. *Neuroscience* 46, 851–857.
- Berland, K.M., So, P.T., Gratton, E., 1995. Two-photon fluorescence correlation spectroscopy: method and application to the intracellular environment. *Biophys. J.* 68, 694–701.
- Brinkmeier, M., Dörre, K., Stephan, J., Eigen, M., 1999. Two-beam cross-correlation: a method to characterize transport phenomena in micrometer-sized structures. *Anal. Chem.* 71, 609–616. <https://doi.org/10.1021/ac980820i>
- Brocke, L., Chiang, L.W., Wagner, P.D., Schulman, H., 1999. Functional implications of the subunit composition of neuronal CaM kinase II. *J. Biol. Chem.* 274, 22713–22722.
- Chen, H., Farkas, E.R., Webb, W.W., 2008. Chapter 1: In vivo applications of fluorescence correlation spectroscopy. *Methods Cell Biol.* 89, 3–35. [https://doi.org/10.1016/S0091-679X\(08\)00601-8](https://doi.org/10.1016/S0091-679X(08)00601-8)
- Chen, Y., Müller, J.D., Ruan, Q., Gratton, E., 2002. Molecular brightness characterization of EGFP in vivo by fluorescence fluctuation spectroscopy. *Biophys. J.* 82, 133–144.
[https://doi.org/10.1016/S0006-3495\(02\)75380-0](https://doi.org/10.1016/S0006-3495(02)75380-0)

- Chen, Y., Müller, J.D., Tetin, S.Y., Tyner, J.D., Gratton, E., 2000. Probing ligand protein binding equilibria with fluorescence fluctuation spectroscopy. *Biophys. J.* 79, 1074–1084.
- Cimler, B.M., Andreasen, T.J., Andreasen, K.I., Storm, D.R., 1985. P-57 is a neural specific calmodulin-binding protein. *J. Biol. Chem.* 260, 10784–10788.
- Cohen, S.M., Li, B., Tsien, R.W., Ma, H., 2015. Evolutionary and functional perspectives on signaling from neuronal surface to nucleus. *Biochem. Biophys. Res. Commun.* 460, 88–99. <https://doi.org/10.1016/j.bbrc.2015.02.146>
- De Koninck, P., Schulman, H., 1998. Sensitivity of CaM kinase II to the frequency of Ca²⁺ oscillations. *Science* 279, 227–230.
- Digman, M.A., Brown, C.M., Sengupta, P., Wiseman, P.W., Horwitz, A.R., Gratton, E., 2005. Measuring fast dynamics in solutions and cells with a laser scanning microscope. *Biophys. J.* 89, 1317–1327. <https://doi.org/10.1529/biophysj.105.062836>
- Dittrich, P.S., Schwille, P., 2002. Spatial two-photon fluorescence cross-correlation spectroscopy for controlling molecular transport in microfluidic structures. *Anal. Chem.* 74, 4472–4479.
- Dosemeci, A., Reese, T.S., Petersen, J., Tao-Cheng, J.H., 2000. A novel particulate form of Ca(2+)/calmodulin-dependent [correction of Ca(2+)/CaMKII-dependent] protein kinase II in neurons. *J. Neurosci. Off. J. Soc. Neurosci.* 20, 3076–3084.
- Fink, C.C., Meyer, T., 2002. Molecular mechanisms of CaMKII activation in neuronal plasticity. *Curr. Opin. Neurobiol.* 12, 293–299.
- Gerendasy, D., 1999. Homeostatic tuning of Ca²⁺ signal transduction by members of the calpacitin protein family. *J. Neurosci. Res.* 58, 107–119.
- Goll, D.E., Thompson, V.F., Li, H., Wei, W., Cong, J., 2003. The calpain system. *Physiol. Rev.* 83, 731–801. <https://doi.org/10.1152/physrev.00029.2002>
- Goshima, N., Kawamura, Y., Fukumoto, A., Miura, A., Honma, R., Satoh, R., Wakamatsu, A., Yamamoto, J., Kimura, K., Nishikawa, T., Andoh, T., Iida, Y., Ishikawa, K., Ito, E., Kagawa, N., Kaminaga, C., Kanehori, K., Kawakami, B., Kenmochi, K., Kimura, R., Kobayashi, M., Kuroita, T., Kuwayama, H., Maruyama, Y., Matsuo, K., Minami, K., Mitsubori, M., Mori, M., Morishita, R., Murase, A., Nishikawa, A., Nishikawa, S., Okamoto, T., Sakagami, N., Sakamoto, Y., Sasaki, Y., Seki, T., Sono, S., Sugiyama, A., Sumiya, T., Takayama, T., Takayama, Y., Takeda, H., Togashi, T., Yahata, K., Yamada, H., Yanagisawa, Y., Endo, Y., Imamoto, F., Kisu, Y., Tanaka, S., Isogai, T., Imai, J., Watanabe, S., Nomura, N., 2008. Human protein factory for converting the transcriptome into an in vitro-expressed proteome. *Nat. Methods* 5, 1011–1017.
- Grant, P.A.A., Best, S.L., Sanmugalingam, N., Alessio, R., Jama, A.M., Török, K., 2008. A two-state model for Ca²⁺/CaM-dependent protein kinase II (alphaCaMKII) in response to persistent Ca²⁺ stimulation in hippocampal neurons. *Cell Calcium* 44, 465–478. <https://doi.org/10.1016/j.ceca.2008.03.003>

- Griffith, L.C., Lu, C.S., Sun, X.X., 2003. CaMKII, an enzyme on the move: regulation of temporospatial localization. *Mol. Interv.* 3, 386–403. <https://doi.org/10.1124/mi.3.7.386>
- Hajimohammadreza, I., Raser, K.J., Nath, R., Nadimpalli, R., Scott, M., Wang, K.K., 1997. Neuronal nitric oxide synthase and calmodulin-dependent protein kinase II α undergo neurotoxin-induced proteolysis. *J. Neurochem.* 69, 1006–1013.
- Haupts, U., Maiti, S., Schwille, P., Webb, W.W., 1998. Dynamics of fluorescence fluctuations in green fluorescent protein observed by fluorescence correlation spectroscopy. *Proc. Natl. Acad. Sci. U. S. A.* 95, 13573–13578.
- Håvik, B., Røkke, H., Bårdsen, K., Davanger, S., Bramham, C.R., 2003. Bursts of high-frequency stimulation trigger rapid delivery of pre-existing α -CaMKII mRNA to synapses: a mechanism in dendritic protein synthesis during long-term potentiation in adult awake rats. *Eur. J. Neurosci.* 17, 2679–2689.
- Hayashi, Y., Shi, S.H., Esteban, J.A., Piccini, A., Poncer, J.C., Malinow, R., 2000. Driving AMPA receptors into synapses by LTP and CaMKII: requirement for GluR1 and PDZ domain interaction. *Science* 287, 2262–2267.
- Heikal, A.A., Hess, S.T., Baird, G.S., Tsien, R.Y., Webb, W.W., 2000. Molecular spectroscopy and dynamics of intrinsically fluorescent proteins: coral red (dsRed) and yellow (Citrine). *Proc. Natl. Acad. Sci. U. S. A.* 97, 11996–12001. <https://doi.org/10.1073/pnas.97.22.11996>
- Heist, E.K., Schulman, H., 1998. The role of Ca²⁺/calmodulin-dependent protein kinases within the nucleus. *Cell Calcium* 23, 103–114.
- Hell, J.W., 2014. CaMKII: claiming center stage in postsynaptic function and organization. *Neuron* 81, 249–265. <https://doi.org/10.1016/j.neuron.2013.12.024>
- Hoelz, A., Nairn, A.C., Kuriyan, J., 2003. Crystal structure of a tetradecameric assembly of the association domain of Ca²⁺/calmodulin-dependent kinase II. *Mol. Cell* 11, 1241–1251.
- Hudmon, A., Aronowski, J., Kolb, S.J., Waxham, M.N., 1996. Inactivation and self-association of Ca²⁺/calmodulin-dependent protein kinase II during autophosphorylation. *J. Biol. Chem.* 271, 8800–8808.
- Hudmon, A., Lebel, E., Roy, H., Sik, A., Schulman, H., Waxham, M.N., De Koninck, P., 2005. A mechanism for Ca²⁺/calmodulin-dependent protein kinase II clustering at synaptic and nonsynaptic sites based on self-association. *J. Neurosci. Off. J. Soc. Neurosci.* 25, 6971–6983. <https://doi.org/10.1523/JNEUROSCI.4698-04.2005>
- Hudmon, A., Schulman, H., 2002a. Structure-function of the multifunctional Ca²⁺/calmodulin-dependent protein kinase II. *Biochem. J.* 364, 593–611. <https://doi.org/10.1042/BJ20020228>
- Hudmon, A., Schulman, H., 2002b. Neuronal CA²⁺/calmodulin-dependent protein kinase II: the role of structure and autoregulation in cellular function. *Annu. Rev. Biochem.* 71, 473–510. <https://doi.org/10.1146/annurev.biochem.71.110601.135410>

- Johnson, C.K., Harms, G.S., 2016. Tracking and localization of calmodulin in live cells. *Biochim. Biophys. Acta* 1863, 2017–2026. <https://doi.org/10.1016/j.bbamcr.2016.04.021>
- Kanaseki, T., Ikeuchi, Y., Sugiura, H., Yamauchi, T., 1991. Structural features of Ca²⁺/calmodulin-dependent protein kinase II revealed by electron microscopy. *J. Cell Biol.* 115, 1049–1060.
- Kerchner, G.A., Nicoll, R.A., 2008. Silent synapses and the emergence of a postsynaptic mechanism for LTP. *Nat. Rev. Neurosci.* 9, 813–825. <https://doi.org/10.1038/nrn2501>
- Khan, S., Reese, T.S., Rajpoot, N., Shabbir, A., 2012. Spatiotemporal maps of CaMKII in dendritic spines. *J. Comput. Neurosci.* 33, 123–139. <https://doi.org/10.1007/s10827-011-0377-1>
- Kim, M.-J., Jo, D.-G., Hong, G.-S., Kim, B.J., Lai, M., Cho, D.-H., Kim, K.-W., Bandyopadhyay, A., Hong, Y.-M., Kim, D.H., Cho, C., Liu, J.O., Snyder, S.H., Jung, Y.-K., 2002. Calpain-dependent cleavage of cain/cabin1 activates calcineurin to mediate calcium-triggered cell death. *Proc. Natl. Acad. Sci. U. S. A.* 99, 9870–9875. <https://doi.org/10.1073/pnas.152336999>
- Kim, S.A., Heinze, K.G., Schwille, P., 2007. Fluorescence correlation spectroscopy in living cells. *Nat. Methods* 4, 963–973. <https://doi.org/10.1038/nmeth1104>
- Kim, S.A., Heinze, K.G., Waxham, M.N., Schwille, P., 2004. Intracellular calmodulin availability accessed with two-photon cross-correlation. *Proc. Natl. Acad. Sci. U. S. A.* 101, 105–110. <https://doi.org/10.1073/pnas.2436461100>
- Kim, S.A., Sanabria, H., Digman, M.A., Gratton, E., Schwille, P., Zipfel, W.R., Waxham, M.N., 2010. Quantifying translational mobility in neurons: comparison between current optical techniques. *J. Neurosci. Off. J. Soc. Neurosci.* 30, 16409–16416. <https://doi.org/10.1523/JNEUROSCI.3063-10.2010>
- Kloster-Landsberg, M., Herbomel, G., Wang, I., Derouard, J., Vourc'h, C., Usson, Y., Souchier, C., Delon, A., 2012. Cellular Response to Heat Shock Studied by Multiconfocal Fluorescence Correlation Spectroscopy. *Biophys. J.* 103, 1110–1119. <https://doi.org/10.1016/j.bpj.2012.07.041>
- Kolb, S.J., Hudmon, A., Ginsberg, T.R., Waxham, M.N., 1998. Identification of domains essential for the assembly of calcium/calmodulin-dependent protein kinase II holoenzymes. *J. Biol. Chem.* 273, 31555–31564.
- Kolodziej, S.J., Hudmon, A., Waxham, M.N., Stoops, J.K., 2000. Three-dimensional reconstructions of calcium/calmodulin-dependent (CaM) kinase II α and truncated CaM kinase II α reveal a unique organization for its structural core and functional domains. *J. Biol. Chem.* 275, 14354–14359.
- Kutcher, L.W., Beauman, S.R., Gruenstein, E.I., Kaetzel, M.A., Dedman, J.R., 2003. Nuclear CaMKII inhibits neuronal differentiation of PC12 cells without affecting MAPK or CREB activation. *Am. J. Physiol. Cell Physiol.* 284, C1334–1345. <https://doi.org/10.1152/ajpcell.00510.2002>

- Kwiatkowski, A.P., King, M.M., 1989. Autophosphorylation of the type II calmodulin-dependent protein kinase is essential for formation of a proteolytic fragment with catalytic activity. Implications for long-term synaptic potentiation. *Biochemistry (Mosc.)* 28, 5380–5385.
- Lantsman, K., Tombes, R.M., 2005. CaMK-II oligomerization potential determined using CFP/YFP FRET. *Biochim. Biophys. Acta* 1746, 45–54.
<https://doi.org/10.1016/j.bbamcr.2005.08.005>
- Lee, S.-J.R., Escobedo-Lozoya, Y., Szatmari, E.M., Yasuda, R., 2009. Activation of CaMKII in single dendritic spines during long-term potentiation. *Nature* 458, 299–304.
<https://doi.org/10.1038/nature07842>
- Lin, Y.-C., Redmond, L., 2009. Neuronal CaMKII acts as a structural kinase. *Commun. Integr. Biol.* 2, 40–41.
- Lisman, J., Schulman, H., Cline, H., 2002. The molecular basis of CaMKII function in synaptic and behavioural memory. *Nat. Rev. Neurosci.* 3, 175–190.
<https://doi.org/10.1038/nrn753>
- Lisman, J., Yasuda, R., Raghavachari, S., 2012a. Mechanisms of CaMKII action in long-term potentiation. *Nat. Rev. Neurosci.* 13, 169–182. <https://doi.org/10.1038/nrn3192>
- Lisman, J., Yasuda, R., Raghavachari, S., 2012b. Mechanisms of CaMKII action in long-term potentiation. *Nat. Rev. Neurosci.* 13, 169–182. <https://doi.org/10.1038/nrn3192>
- Lisman, J.E., Zhabotinsky, A.M., 2001. A model of synaptic memory: a CaMKII/PP1 switch that potentiates transmission by organizing an AMPA receptor anchoring assembly. *Neuron* 31, 191–201.
- Liu, M.C., Akle, V., Zheng, W., Dave, J.R., Tortella, F.C., Hayes, R.L., Wang, K.K.W., 2006. Comparing calpain- and caspase-3-mediated degradation patterns in traumatic brain injury by differential proteome analysis. *Biochem. J.* 394, 715–725.
<https://doi.org/10.1042/BJ20050905>
- Lu, H.E., MacGillavry, H.D., Frost, N.A., Blanpied, T.A., 2014. Multiple spatial and kinetic subpopulations of CaMKII in spines and dendrites as resolved by single-molecule tracking PALM. *J. Neurosci. Off. J. Soc. Neurosci.* 34, 7600–7610.
<https://doi.org/10.1523/JNEUROSCI.4364-13.2014>
- Luby-Phelps, K., Hori, M., Phelps, J.M., Won, D., 1995. Ca(2+)-regulated dynamic compartmentalization of calmodulin in living smooth muscle cells. *J. Biol. Chem.* 270, 21532–21538.
- Luby-Phelps, K., Lanni, F., Taylor, D.L., 1985. Behavior of a fluorescent analogue of calmodulin in living 3T3 cells. *J. Cell Biol.* 101, 1245–1256.
- Ma, H., Groth, R.D., Cohen, S.M., Emery, J.F., Li, B., Hoedt, E., Zhang, G., Neubert, T.A., Tsien, R.W., 2014. γ CaMKII shuttles Ca²⁺/CaM to the nucleus to trigger CREB phosphorylation and gene expression. *Cell* 159, 281–294.
<https://doi.org/10.1016/j.cell.2014.09.019>

- Ma, H., Li, B., Tsien, R.W., 2015a. Distinct roles of multiple isoforms of CaMKII in signaling to the nucleus. *Biochim. Biophys. Acta* 1853, 1953–1957.
<https://doi.org/10.1016/j.bbamcr.2015.02.008>
- Ma, H., Li, B., Tsien, R.W., 2015b. Distinct roles of multiple isoforms of CaMKII in signaling to the nucleus. *Biochim. Biophys. Acta* 1853, 1953–1957.
<https://doi.org/10.1016/j.bbamcr.2015.02.008>
- Meissner, O., Häberlein, H., 2003. Lateral mobility and specific binding to GABA(A) receptors on hippocampal neurons monitored by fluorescence correlation spectroscopy. *Biochemistry (Mosc.)* 42, 1667–1672. <https://doi.org/10.1021/bi0263356>
- Merkle, D., Zheng, D., Ohrt, T., Crell, K., Schwille, P., 2008. Cellular dynamics of Ku: characterization and purification of Ku-eGFP. *Chembiochem Eur. J. Chem. Biol.* 9, 1251–1259. <https://doi.org/10.1002/cbic.200700750>
- Merrill, M.A., Chen, Y., Strack, S., Hell, J.W., 2005. Activity-driven postsynaptic translocation of CaMKII. *Trends Pharmacol. Sci.* 26, 645–653.
<https://doi.org/10.1016/j.tips.2005.10.003>
- Mulkey, R.M., Endo, S., Shenolikar, S., Malenka, R.C., 1994. Involvement of a calcineurin/inhibitor-1 phosphatase cascade in hippocampal long-term depression. *Nature* 369, 486–488. <https://doi.org/10.1038/369486a0>
- Müller, J.D., Chen, Y., Gratton, E., 2003. Fluorescence correlation spectroscopy. *Methods Enzymol.* 361, 69–92.
- Myers, J.B., Zaegel, V., Coultrap, S.J., Miller, A.P., Bayer, K.U., Reichow, S.L., 2017. The CaMKII holoenzyme structure in activation-competent conformations. *Nat. Commun.* 8, 15742. <https://doi.org/10.1038/ncomms15742>
- Needleman, D.J., Xu, Y., Mitchison, T.J., 2009. Pin-Hole Array Correlation Imaging: Highly Parallel Fluorescence Correlation Spectroscopy. *Biophys. J.* 96, 5050–5059.
<https://doi.org/10.1016/j.bpj.2009.03.023>
- Nguyen, T.A., Sarkar, P., Veetil, J.V., Davis, K.A., Puhl, H.L., Vogel, S.S., 2015. Covert Changes in CaMKII Holoenzyme Structure Identified for Activation and Subsequent Interactions. *Biophys. J.* 108, 2158–2170. <https://doi.org/10.1016/j.bpj.2015.03.028>
- Ohsugi, Y., Kinjo, M., 2009. Multipoint fluorescence correlation spectroscopy with total internal reflection fluorescence microscope. *J. Biomed. Opt.* 14, 014030.
<https://doi.org/10.1117/1.3080723>
- Otmakhov, N., Tao-Cheng, J.-H., Carpenter, S., Asrican, B., Dosemeci, A., Reese, T.S., Lisman, J., 2004. Persistent accumulation of calcium/calmodulin-dependent protein kinase II in dendritic spines after induction of NMDA receptor-dependent chemical long-term potentiation. *J. Neurosci. Off. J. Soc. Neurosci.* 24, 9324–9331.
<https://doi.org/10.1523/JNEUROSCI.2350-04.2004>

- Ouimet, C.C., Hemmings, H.C., Greengard, P., 1989. ARPP-21, a cyclic AMP-regulated phosphoprotein enriched in dopamine-innervated brain regions. II. Immunocytochemical localization in rat brain. *J. Neurosci. Off. J. Soc. Neurosci.* 9, 865–875.
- Ouyang, Y., Rosenstein, A., Kreiman, G., Schuman, E.M., Kennedy, M.B., 1999. Tetanic stimulation leads to increased accumulation of Ca(2+)/calmodulin-dependent protein kinase II via dendritic protein synthesis in hippocampal neurons. *J. Neurosci. Off. J. Soc. Neurosci.* 19, 7823–7833.
- Petersen, A., Gerges, N.Z., 2015. Neurogranin regulates CaM dynamics at dendritic spines. *Sci. Rep.* 5, 11135. <https://doi.org/10.1038/srep11135>
- Petrásek, Z., Schwille, P., 2008. Precise measurement of diffusion coefficients using scanning fluorescence correlation spectroscopy. *Biophys. J.* 94, 1437–1448. <https://doi.org/10.1529/biophysj.107.108811>
- Price, E.S., Aleksiejew, M., Johnson, C.K., 2011. FRET-FCS detection of intralobe dynamics in calmodulin. *J. Phys. Chem. B* 115, 9320–9326. <https://doi.org/10.1021/jp203743m>
- Price, E.S., DeVore, M.S., Johnson, C.K., 2010. Detecting intramolecular dynamics and multiple Förster resonance energy transfer states by fluorescence correlation spectroscopy. *J. Phys. Chem. B* 114, 5895–5902. <https://doi.org/10.1021/jp912125z>
- Rakhilin, S.V., Olson, P.A., Nishi, A., Starkova, N.N., Fienberg, A.A., Nairn, A.C., Surmeier, D.J., Greengard, P., 2004. A network of control mediated by regulator of calcium/calmodulin-dependent signaling. *Science* 306, 698–701. <https://doi.org/10.1126/science.1099961>
- Ries, J., Chiantia, S., Schwille, P., 2009. Accurate determination of membrane dynamics with line-scan FCS. *Biophys. J.* 96, 1999–2008. <https://doi.org/10.1016/j.bpj.2008.12.3888>
- Rostas, J.A., Dunkley, P.R., 1992. Multiple forms and distribution of calcium/calmodulin-stimulated protein kinase II in brain. *J. Neurochem.* 59, 1191–1202.
- Ruan, Q., Cheng, M.A., Levi, M., Gratton, E., Mantulin, W.W., 2004. Spatial-temporal studies of membrane dynamics: scanning fluorescence correlation spectroscopy (SFCS). *Biophys. J.* 87, 1260–1267. <https://doi.org/10.1529/biophysj.103.036483>
- Sanabria, H., Digman, M.A., Gratton, E., Waxham, M.N., 2008. Spatial diffusivity and availability of intracellular calmodulin. *Biophys. J.* 95, 6002–6015. <https://doi.org/10.1529/biophysj.108.138974>
- Sanabria, H., Kubota, Y., Waxham, M.N., 2007. Multiple diffusion mechanisms due to nanostructuring in crowded environments. *Biophys. J.* 92, 313–322. <https://doi.org/10.1529/biophysj.106.090498>
- Sanabria, H., Swilius, M.T., Kolodziej, S.J., Liu, J., Waxham, M.N., 2009. β CaMKII regulates actin assembly and structure. *J. Biol. Chem.* 284, 9770–9780. <https://doi.org/10.1074/jbc.M809518200>

- Sanabria, H., Waxham, M.N., 2010. Transient anomalous subdiffusion: effects of specific and nonspecific probe binding with actin gels. *J. Phys. Chem. B* 114, 959–972. <https://doi.org/10.1021/jp9072153>
- Sanhueza, M., Lisman, J., 2013. The CaMKII/NMDAR complex as a molecular memory. *Mol. Brain* 6, 10. <https://doi.org/10.1186/1756-6606-6-10>
- Schulman, H., Hanson, P.I., 1993. Multifunctional Ca²⁺/calmodulin-dependent protein kinase. *Neurochem. Res.* 18, 65–77.
- Schwille, P., 2001. Fluorescence correlation spectroscopy and its potential for intracellular applications. *Cell Biochem. Biophys.* 34, 383–408. <https://doi.org/10.1385/CBB:34:3:383>
- Schwille, P., Haupts, U., Maiti, S., Webb, W.W., 1999. Molecular dynamics in living cells observed by fluorescence correlation spectroscopy with one- and two-photon excitation. *Biophys. J.* 77, 2251–2265. [https://doi.org/10.1016/S0006-3495\(99\)77065-7](https://doi.org/10.1016/S0006-3495(99)77065-7)
- Schwille, P., Haustein, E., 2006. Fluorescence Correlation Spectroscopy - An Introduction to its Concepts and Applications. <https://doi.org/10.1002/lpor.200910041>
- Shafeghat, N., Heidarinejad, M., Murata, N., Nakamura, H., Inoue, T., 2016. Optical detection of neuron connectivity by random access two-photon microscopy. *J. Neurosci. Methods* 263, 48–56. <https://doi.org/10.1016/j.jneumeth.2016.01.023>
- Shen, K., Meyer, T., 1999. Dynamic control of CaMKII translocation and localization in hippocampal neurons by NMDA receptor stimulation. *Science* 284, 162–166.
- Shen, K., Meyer, T., 1998. In vivo and in vitro characterization of the sequence requirement for oligomer formation of Ca²⁺/calmodulin-dependent protein kinase IIalpha. *J. Neurochem.* 70, 96–104.
- Shen, K., Teruel, M.N., Subramanian, K., Meyer, T., 1998. CaMKIIbeta functions as an F-actin targeting module that localizes CaMKIIalpha/beta heterooligomers to dendritic spines. *Neuron* 21, 593–606.
- Slade, K.M., Baker, R., Chua, M., Thompson, N.L., Pielak, G.J., 2009. Effects of recombinant protein expression on green fluorescent protein diffusion in *Escherichia coli*. *Biochemistry (Mosc.)* 48, 5083–5089. <https://doi.org/10.1021/bi9004107>
- Srinivasan, M., Edman, C.F., Schulman, H., 1994. Alternative splicing introduces a nuclear localization signal that targets multifunctional CaM kinase to the nucleus. *J. Cell Biol.* 126, 839–852.
- Takeuchi, Y., Fukunaga, K., Miyamoto, E., 2002. Activation of nuclear Ca(2+)/calmodulin-dependent protein kinase II and brain-derived neurotrophic factor gene expression by stimulation of dopamine D2 receptor in transfected NG108-15 cells. *J. Neurochem.* 82, 316–328.
- Takeuchi, Y., Yamamoto, H., Fukunaga, K., Miyakawa, T., Miyamoto, E., 2000. Identification of the isoforms of Ca(2+)/Calmodulin-dependent protein kinase II in rat astrocytes and their subcellular localization. *J. Neurochem.* 74, 2557–2567.

- Tao-Cheng, J.H., Vinade, L., Smith, C., Winters, C.A., Ward, R., Brightman, M.W., Reese, T.S., Dosemeci, A., 2001. Sustained elevation of calcium induces Ca(2+)/calmodulin-dependent protein kinase II clusters in hippocampal neurons. *Neuroscience* 106, 69–78.
- Tremper-Wells, B., Vallano, M.L., 2005. Nuclear calpain regulates Ca²⁺-dependent signaling via proteolysis of nuclear Ca²⁺/calmodulin-dependent protein kinase type IV in cultured neurons. *J. Biol. Chem.* 280, 2165–2175. <https://doi.org/10.1074/jbc.M410591200>
- Watanabe, N., Mitchison, T.J., 2002. Single-molecule speckle analysis of actin filament turnover in lamellipodia. *Science* 295, 1083–1086. <https://doi.org/10.1126/science.1067470>
- Watson, J.B., Sutcliffe, J.G., Fisher, R.S., 1992. Localization of the protein kinase C phosphorylation/calmodulin-binding substrate RC3 in dendritic spines of neostriatal neurons. *Proc. Natl. Acad. Sci. U. S. A.* 89, 8581–8585.
- Wohland, T., Rigler, R., Vogel, H., 2001. The standard deviation in fluorescence correlation spectroscopy. *Biophys. J.* 80, 2987–2999. [https://doi.org/10.1016/S0006-3495\(01\)76264-9](https://doi.org/10.1016/S0006-3495(01)76264-9)
- Xia, Z., Storm, D.R., 2005. The role of calmodulin as a signal integrator for synaptic plasticity. *Nat. Rev. Neurosci.* 6, 267–276. <https://doi.org/10.1038/nrn1647>
- Yang, F., Moss, L.G., Phillips, G.N., 1996. The molecular structure of green fluorescent protein. *Nat. Biotechnol.* 14, 1246–1251. <https://doi.org/10.1038/nbt1096-1246>
- Yasuda, H., Higashi, H., Kudo, Y., Inoue, T., Hata, Y., Mikoshiba, K., Tsumoto, T., 2003. Imaging of calcineurin activated by long-term depression-inducing synaptic inputs in living neurons of rat visual cortex. *Eur. J. Neurosci.* 17, 287–297.
- Yoshimura, Y., Nomura, T., Yamauchi, T., 1996. Purification and characterization of active fragment of Ca²⁺/calmodulin-dependent protein kinase II from the post-synaptic density in the rat forebrain. *J. Biochem. (Tokyo)* 119, 268–273.
- Zacharias, D.A., Violin, J.D., Newton, A.C., Tsien, R.Y., 2002. Partitioning of lipid-modified monomeric GFPs into membrane microdomains of live cells. *Science* 296, 913–916. <https://doi.org/10.1126/science.1068539>
- Zhou, H.-X., Rivas, G., Minton, A.P., 2008. Macromolecular crowding and confinement: biochemical, biophysical, and potential physiological consequences. *Annu. Rev. Biophys.* 37, 375–397. <https://doi.org/10.1146/annurev.biophys.37.032807.125817>

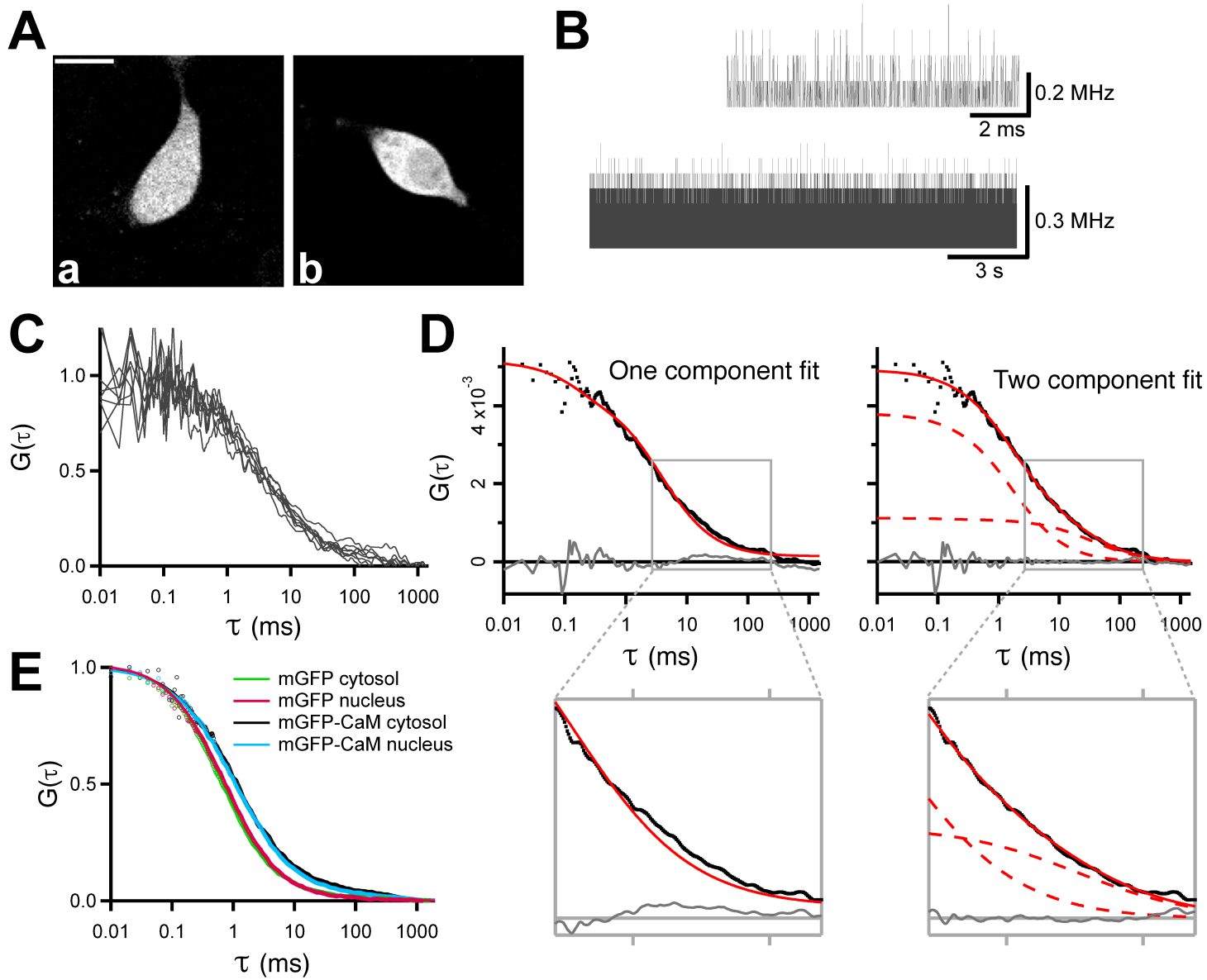


Fig. 1. Heidarinejad et al.

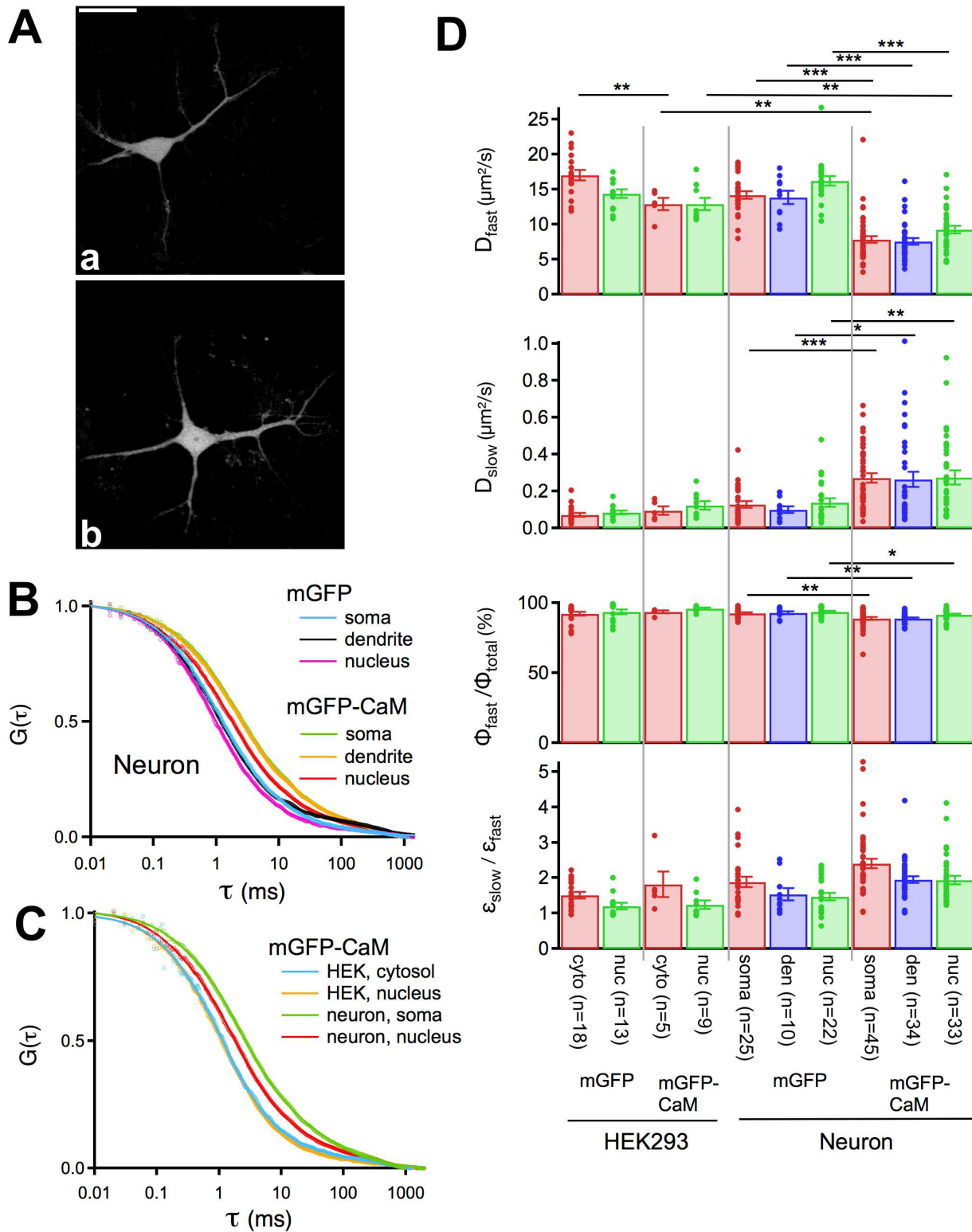


Fig. 2. Heidarinejad et al.

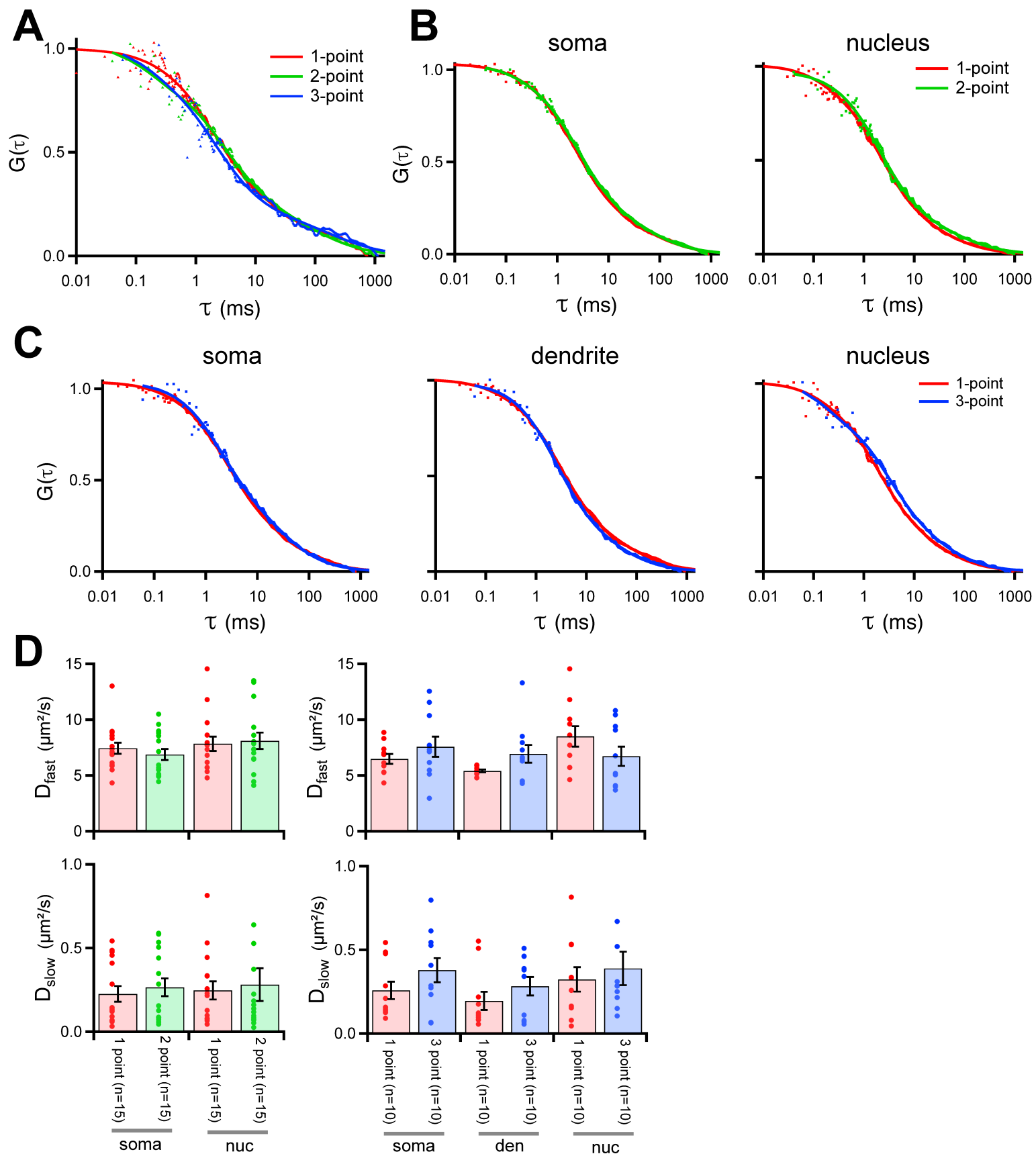


Fig 3. Heidarinejad et al.

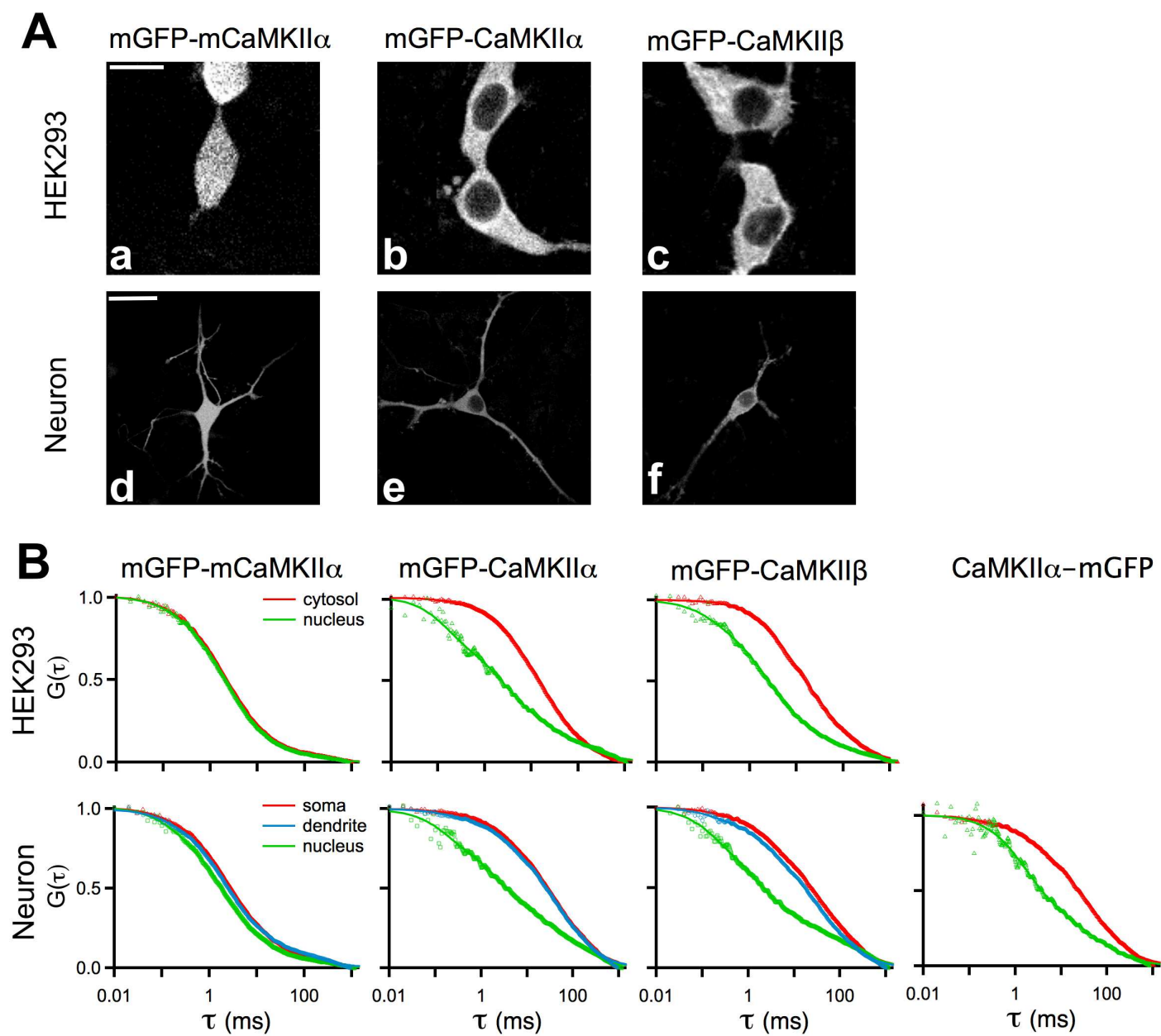


Fig 4. Heidarinejad et al.

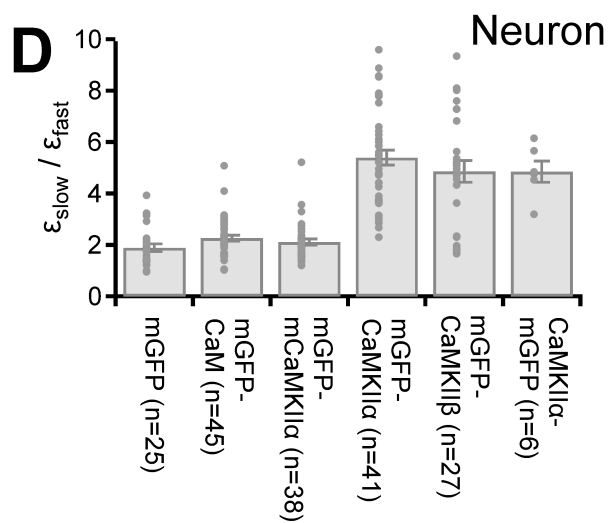
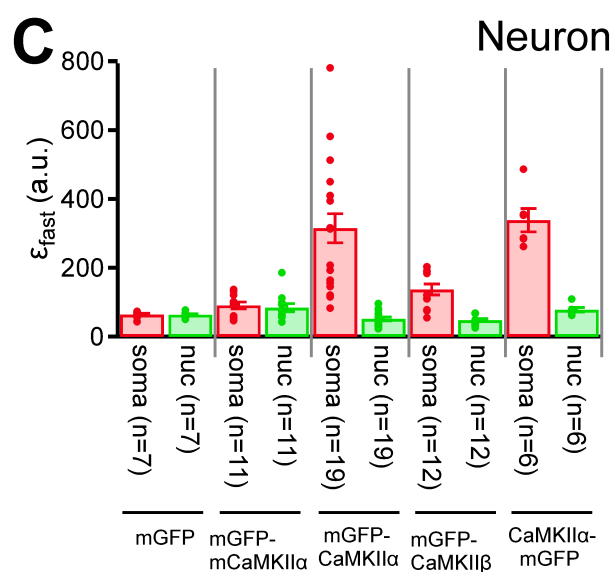
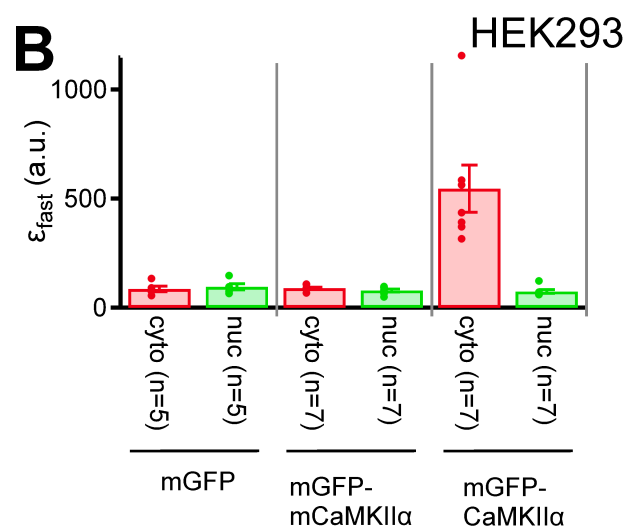
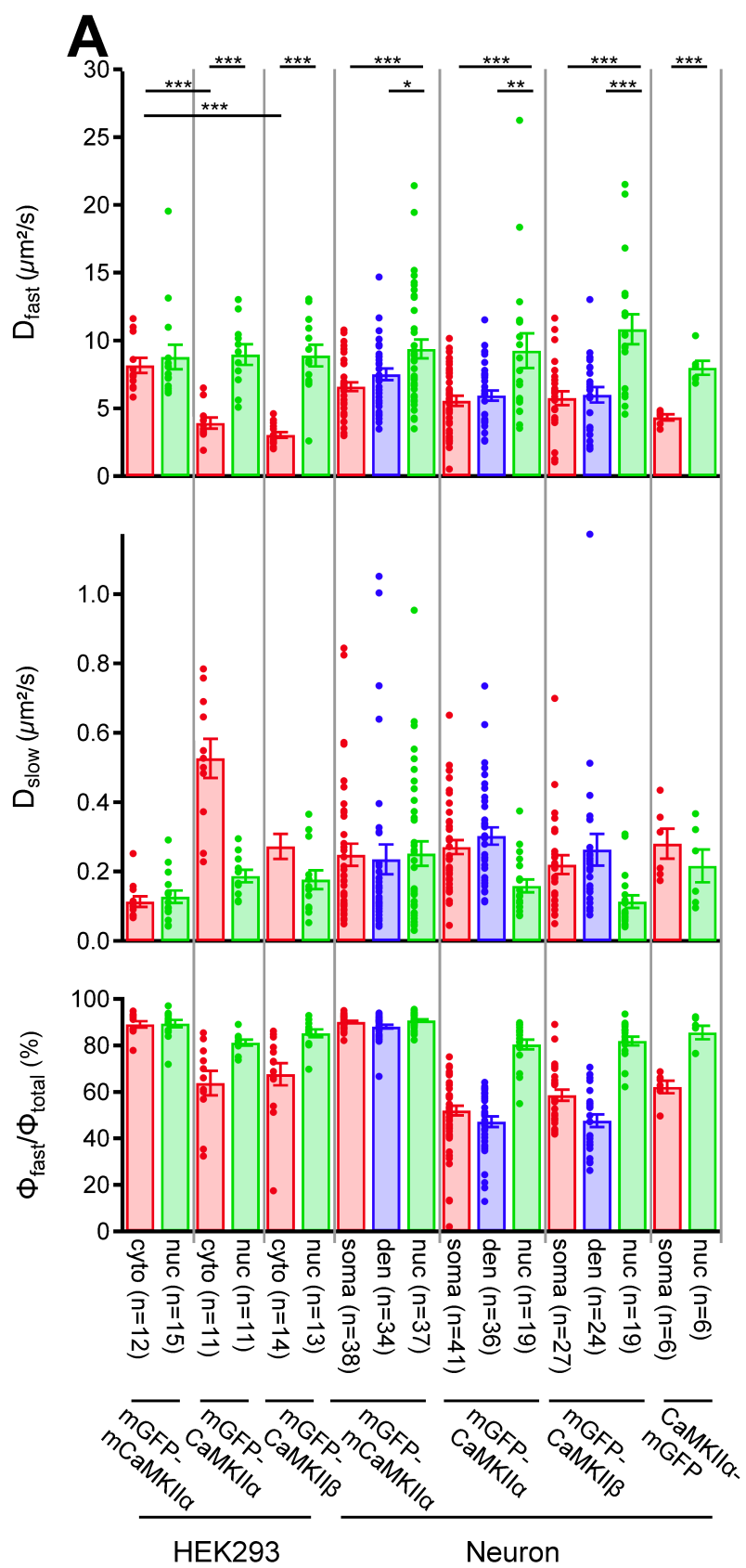


Fig. 5 Heidarinejad et al.

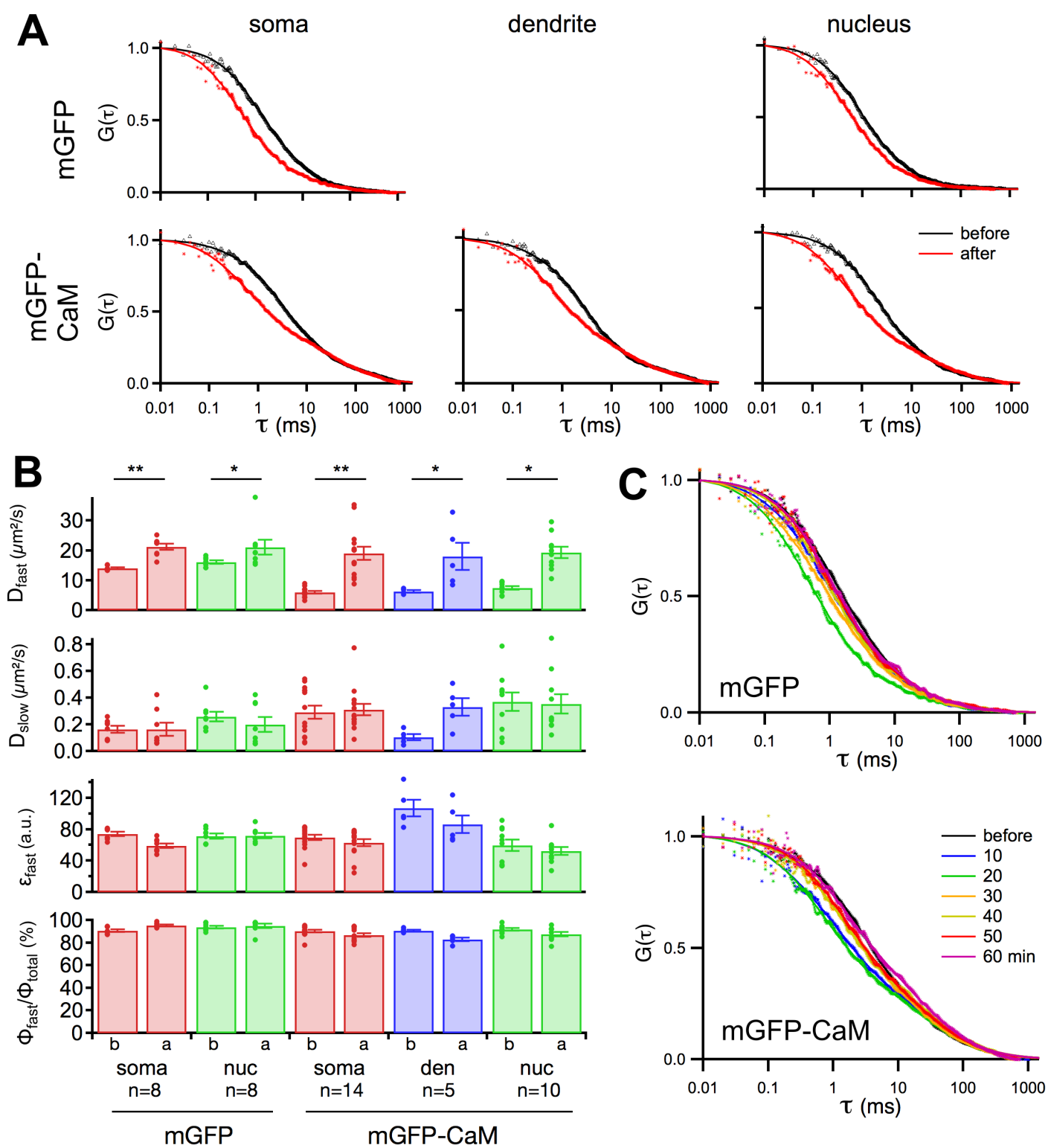


Fig. 6. Heidarinejad et al.

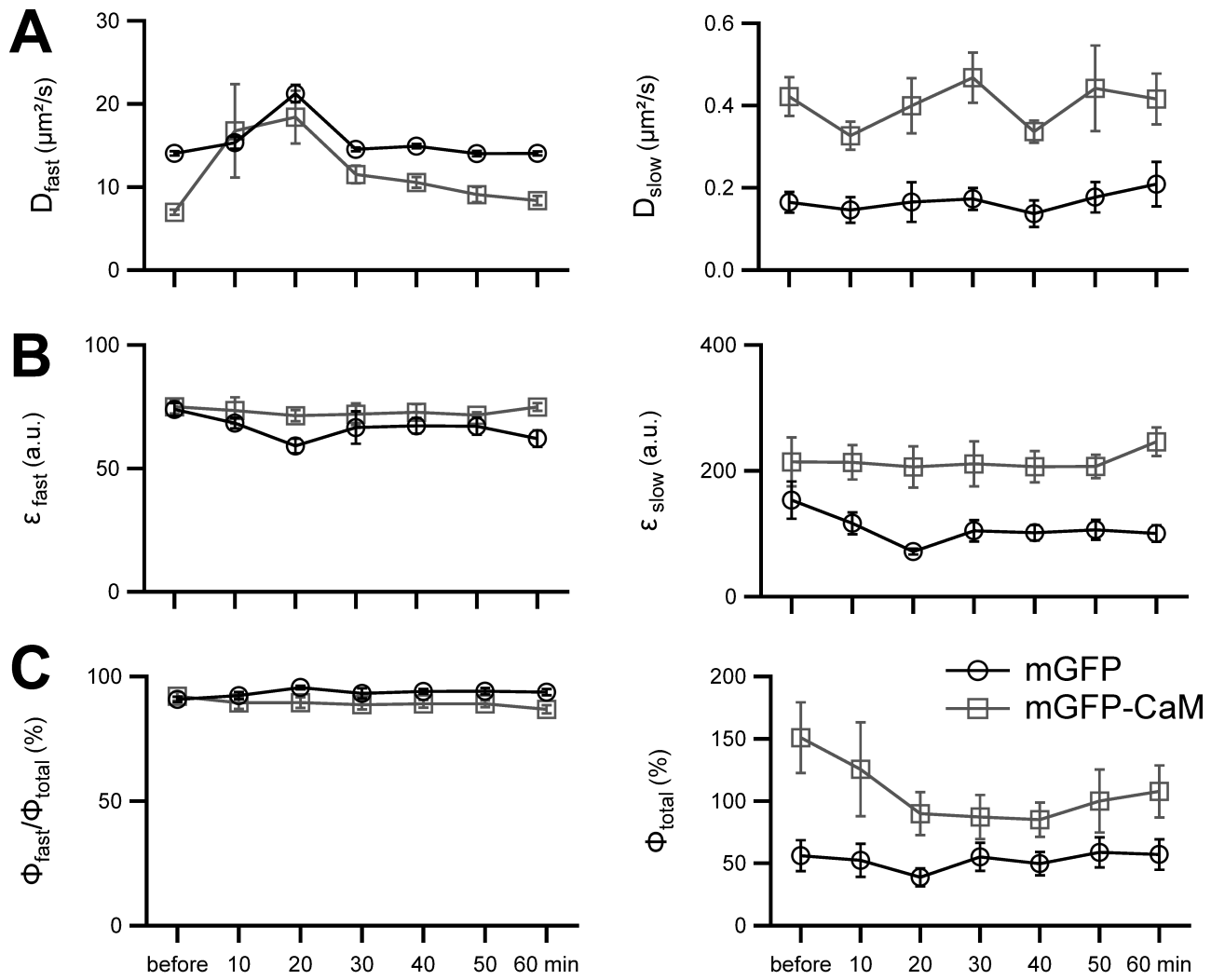


Fig. 7. Heidarinejad et al.

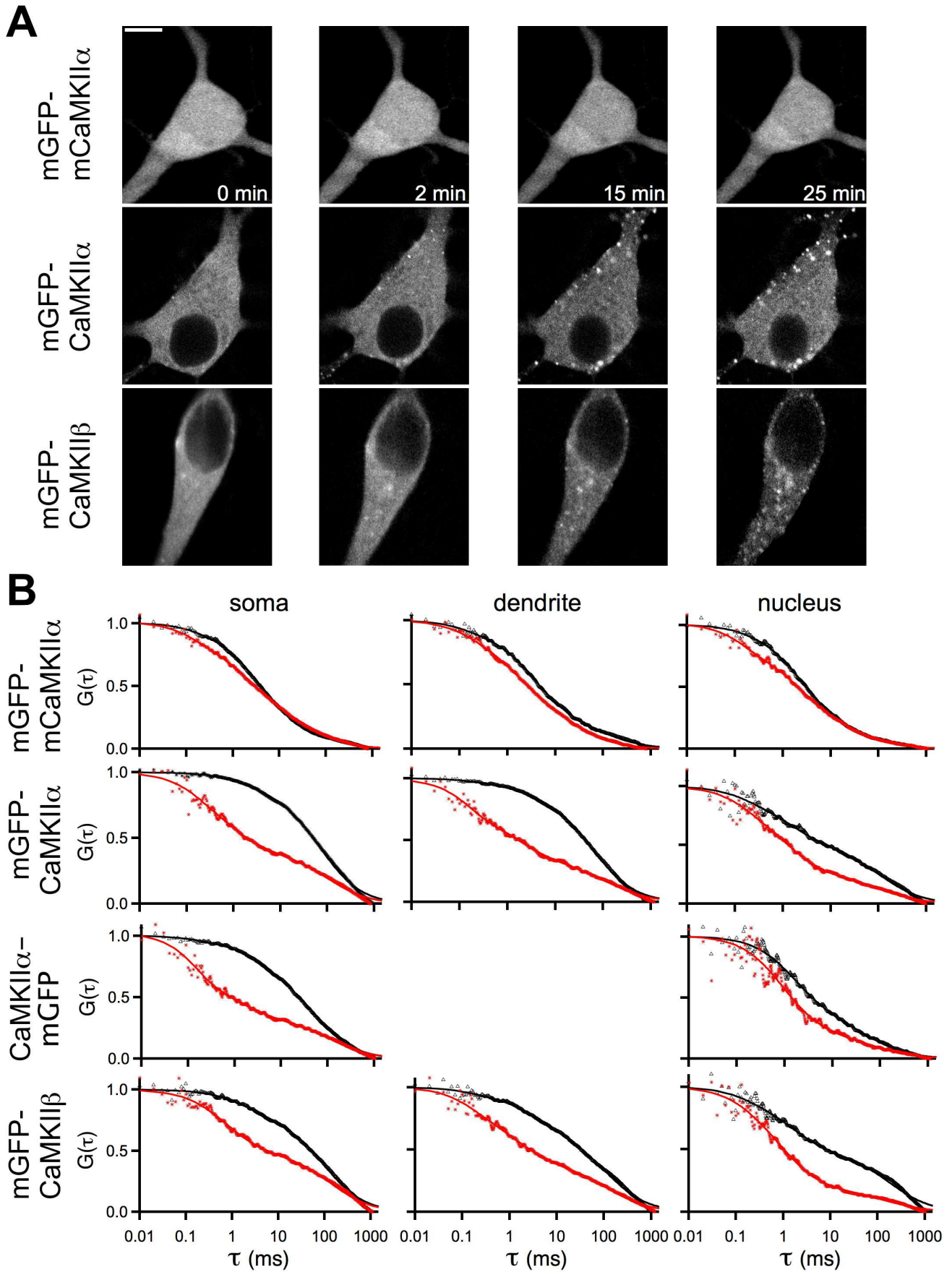


Fig. 8. Heidarinejad et al.

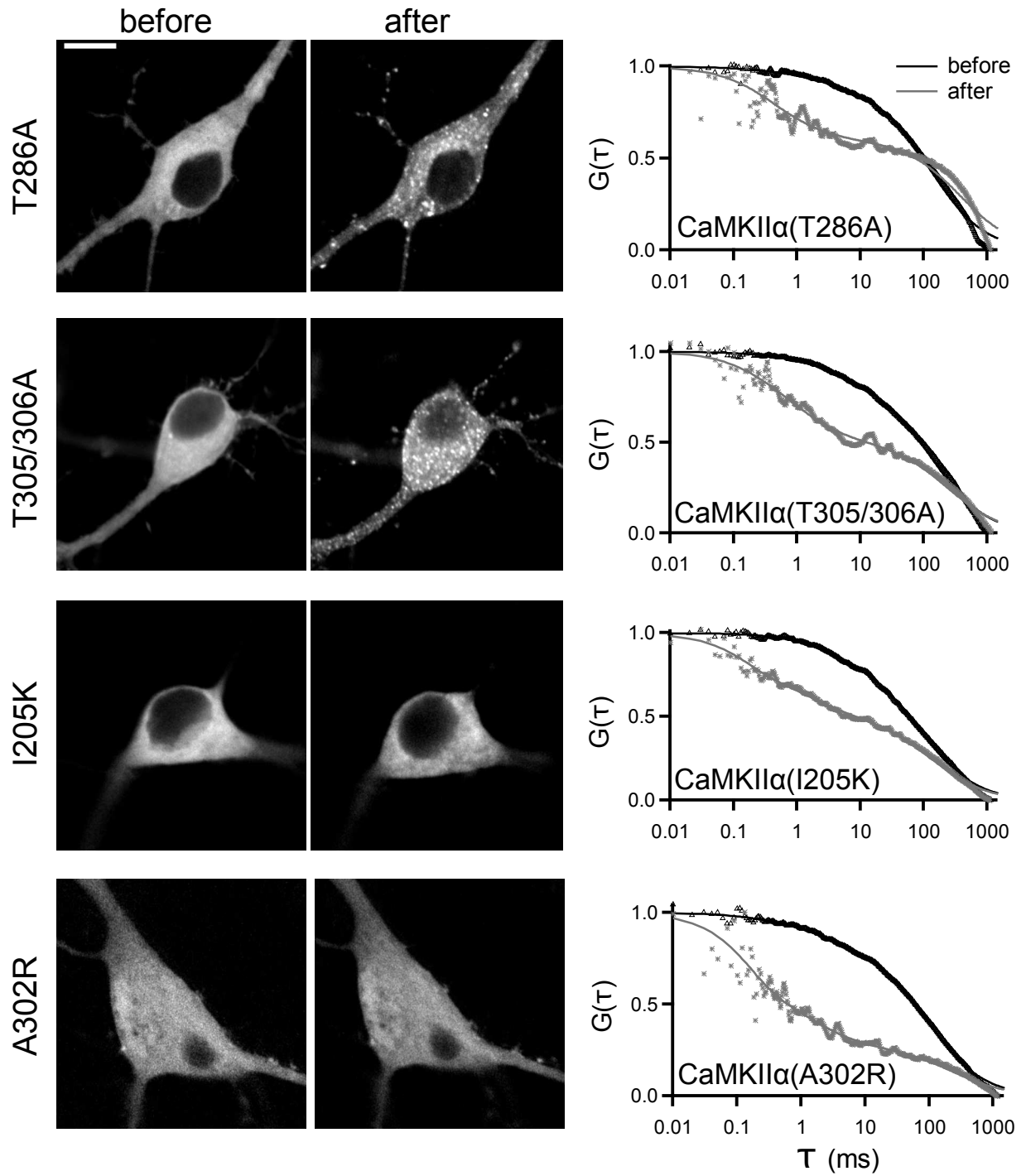


Fig. 9. Heidarinejad et al.

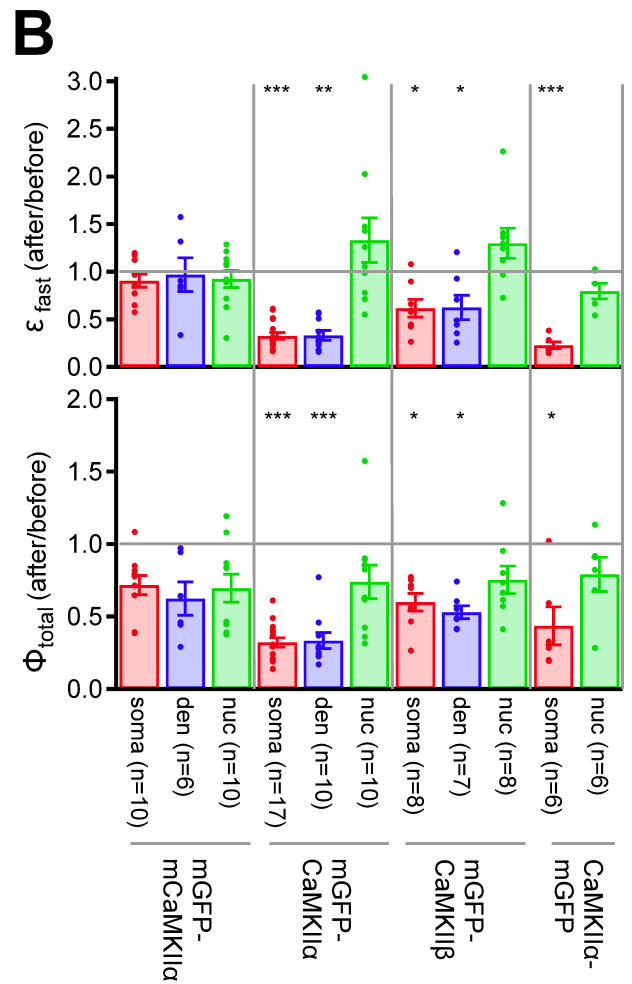
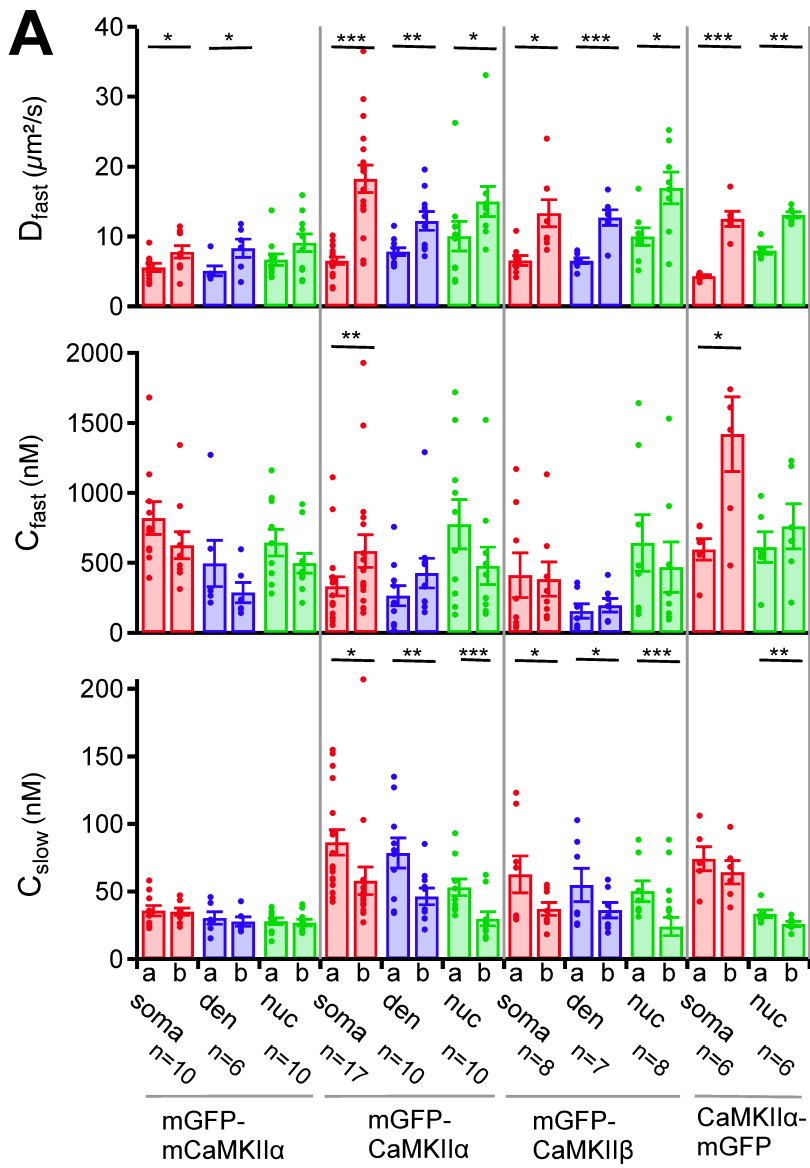


Fig. 10 Heidarinejad et al.

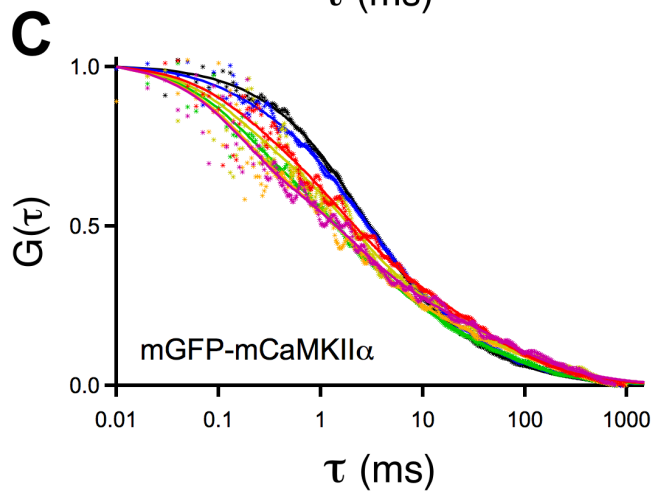
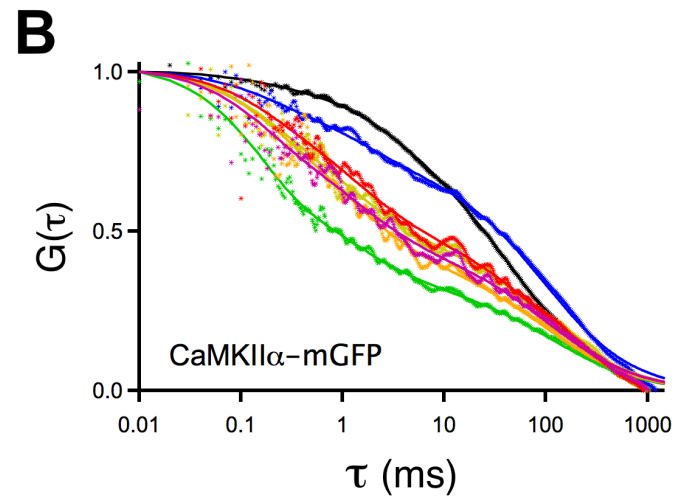
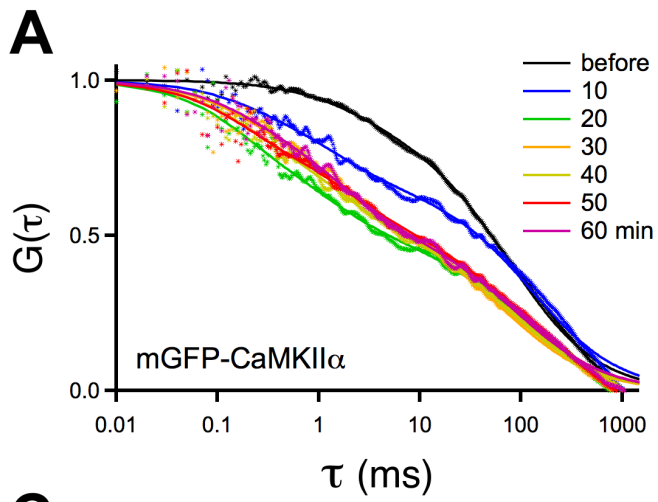


Fig. 11. Heidarinejad et al.

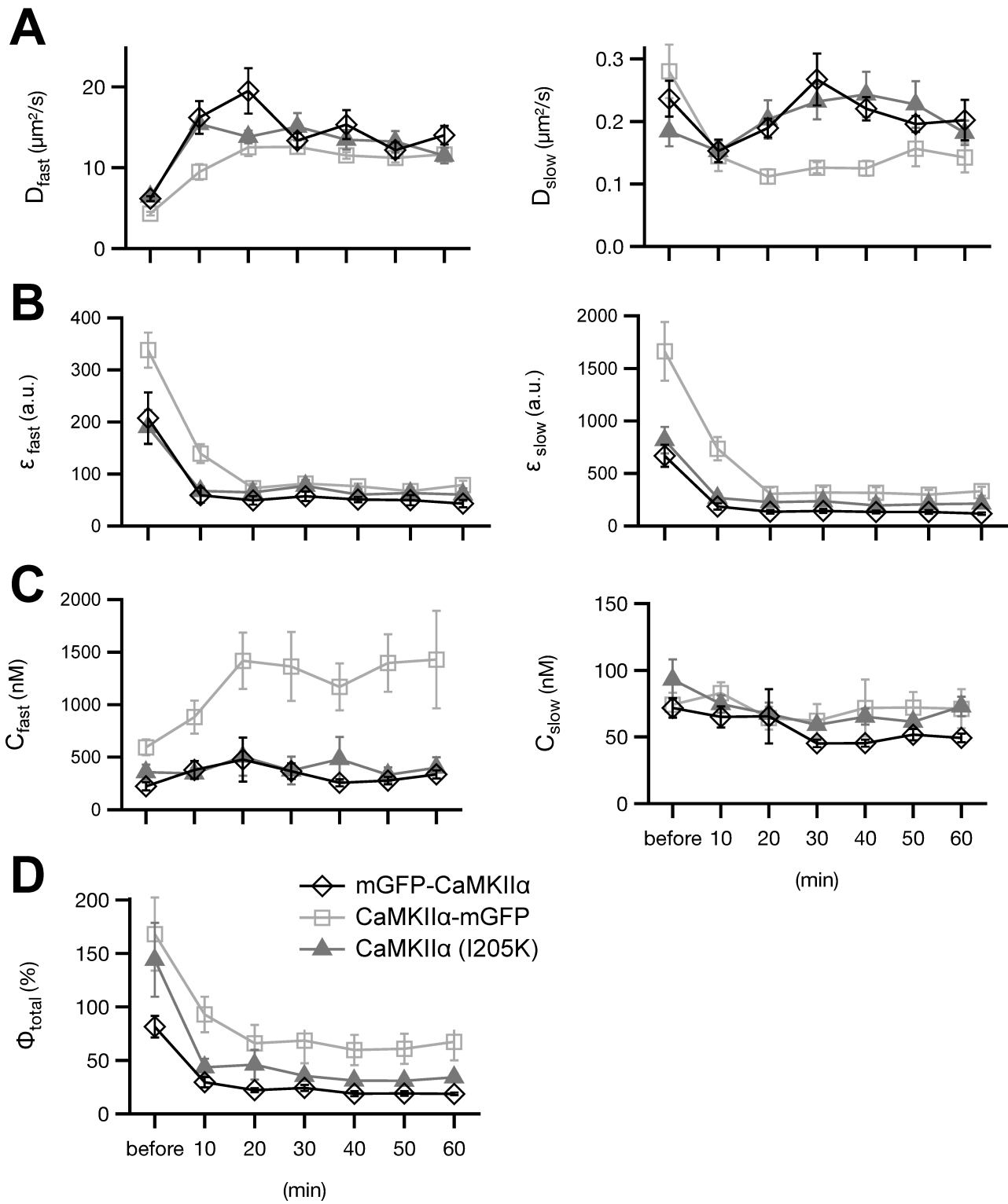


Fig. 12. Heidarinejad et al.